Elsevier Editorial System(tm) for
Palaeogeography, Palaeoclimatology, Palaeoecology
Manuscript Draft

Manuscript Number: PALAEO8460R2

Title: Central Mediterranean Mid-Pleistocene paleoclimatic variability and its association with global climate

Article Type: Research Paper

Keywords: Planktonic foraminifera; Middle Pleistocene; Central Mediterranean; Paleoceanographic changes

Corresponding Author: Dr. Lucilla Capotondi, Ph.D.

Corresponding Author's Institution: National Research Council

First Author: Lucilla Capotondi, Ph.D.

Order of Authors: Lucilla Capotondi, Ph.D.; Angela Girone; Fabrizio Lirer; Caterina Bergami; Marina Verducci; Mattia Vallefuoco; Angelica Afferri; Luciana Ferraro; Nicola Pelosi; Gert J De Lange

Abstract: Planktonic foraminiferal assemblages were studied at high-resolution in core KC01B from the Ionian Sea. Quantitative analysis allowed us to distinguish the main climatic features and associated paleoceanographic changes, that occurred between Marine Isotopic Stages (MIS) 13 and 9 (~ 500-300 ka).
MIS 12 and MIS 10 are characterized by relatively temperate conditions and an oligotrophic oceanographic regime in the early part and by colder conditions and nutrient supply in the sub-surface water masses in the upper part. During these intervals, small but distinct peaks of Neogloboquadrina pachyderma sinistral (sin) are detected at times of extremely negative values of the planktonic foraminifera paleoclimatic curve. Their co-occurrence with similar episodes in the Atlantic suggests that the climate in the Central Mediterranean was associated with north-Atlantic millennial-scale climate instability. MIS 11 and MIS 9 are dominated by surficial warm-water taxa. The climate optimum is reached in the middle part of each of these stages, as denoted by the presence of Globigerinoides sacculifer, and persists for approximately 20 and 6 ka during MIS 11 and MIS 9 respectively. This warming is not constant but is characterized by three distinct intervals with elevated winter temperatures and/or weak winter mixing.
Distribution of Globigerina bulloides, Turborotalita quinqueloba and Neogloboquadrina pachyderma dextral (dex) indicates that significant environmental changes occur across the transitions from glacial to interglacial MIS 12/MIS 11 (Termination V) and MIS 10/MIS 9 (Termination IV).
The studied record documents a close linkage between Mediterranean climate evolution and higher- and lower-latitude climate change throughout MIS 13-9.

Cover Letter, for Editor only

November, 2, 2015

Dear Editor,

I attach you the revised version of the manuscript entitled "*Central Mediterranean Mid-Pleistocene paleoclimatic variability and its association with global climate*" submitted by Lucilla Capotondi, Angela Girone, Fabrizio Lirer, Caterina Bergami, Marina Verducci, Mattia Vallefuoco, Angelica Afferri, Luciana Ferraro, Nicola Pelosi, Gert J De Lange. (REF PALAEO8460R1).

The "*apparently minor mistakes*" evidenced by the referee have been corrected. However I realized that the mistakes (many words linked without spaces between them) present in the pdf version are not present in the submitted Word version. The changes are in the file.pdf generated by the system. I think this is due to the fact that I have submitted the manuscript as a file "word.docx" and not "word.doc". I'm warning that probably the system does not convert well the version word.docx.

I add the point to point response to the reviewers, a version of the revised manuscript showing the new/changed text and a clean version of the revised manuscript.

Kind Regards

Lucilla Capotondi

Highlights

High-resolution Mid-Pleistocene climate reconstruction in the Central Mediterranean.

Significant changes in temperature and productivity occurred during MISs 12 and 10.

The climatic optimum during MIS 11c shows three warmest phases

T-V and T-IV are characterized by complex paleoceanographic changes

Central Mediterranean Mid-Pleistocene paleoclimatic variability and its association with global climate

Lucilla Capotondi[1*], Angela Girone[2], Fabrizio Lirer [3], Caterina Bergami[1,4], Marina Verducci[5], Mattia Vallefuoco[3], Angelica Afferri[2], Luciana Ferraro[3], Nicola Pelosi[3], Gert J. De Lange[6]

1) CNR - Istituto Scienze Marine (ISMAR) - Via Gobetti 101, 40129 Bologna, Italia

2) Dipartimento di Scienze della Terra e Geoambientali, Università di Bari Aldo Moro, Italia

3) CNR - Istituto per l'Ambiente Marino Costiero (IAMC) - Calata Porta di Massa, Interno Porto di Napoli, 80133, Napoli, Italia

4) CNR - Institute of Agro-environmental and Forest Biology (IBAF), Italy

5) Dipartimento di Scienze della Terra, Università di Siena, Italia

6) Department of Earth Sciences - Geochemistry, Faculty of Geosciences, Utrecht University

* corresponding author: lucilla.capotondi@bo.ismar.cnr.it

Keywords: Planktonic foraminifera, Middle Pleistocene, Central Mediterranean, Paleoceanographic changes.

Abstract

Planktonic foraminiferal assemblages were studied at high-resolution in core KC01B from the Ionian Sea. Quantitative analysis allowed us to distinguish the main climatic features and associated paleoceanographic changes, that occurred between Marine Isotopic Stages (MIS) 13 and 9 (~ 500-300 ka).

MIS 12 and MIS 10 are characterized by relatively temperate conditions and an oligotrophic oceanographic regime in the early part and by colder conditions and nutrient supply in the sub-surface water masses in the upper part. During these intervals, small but distinct peaks of *Neogloboquadrina pachyderma* sinistral (sin) are detected at times of extremely negative values of the planktonic foraminifera paleoclimatic curve. Their co-occurrence with similar episodes in the

Atlantic suggests that the climate in the Central Mediterranean was associated with north-Atlantic millennial-scale climate instability. MIS 11 and MIS 9 are dominated by surficial warm-water taxa. The climate optimum is reached in the middle part of each of these stages, as denoted by the presence of *Globigerinoides sacculifer*, and persists for approximately 20 and 6 ka during MIS 11 and MIS 9 respectively. This warming is not constant but is characterized by three distinct intervals with elevated winter temperatures and/or weak winter mixing.

Distribution of *Globigerina bulloides*, *Turborotalita quinqueloba* and *Neogloboquadrina pachyderma* dextral (dex) indicates that significant environmental changes occur across the transitions from glacial to interglacial MIS 12/MIS 11 (Termination V) and MIS 10/MIS 9 (Termination IV).

The studied record documents a close linkage between Mediterranean climate evolution and higher- and lower-latitude climate change throughout MIS 13–9.

1. Introduction

To improve our understanding of natural climate variability and our abilities to forecast future climate change, it is essential to investigate geological climate archives with relevant climate change events. Accordingly, this paper focuses on climate variability that occurred before and after the Mid-Brunhes event (MBE) (Jansen et al., 1986) in the Mediterranean Sea. The investigated time interval (MIS 13-MIS 11; ~ 500-300 ka) is characterized by substantially warmer interglacials, (Epica Members, 2004; Jouzel et al., 2007) and enhanced atmospheric CO_2 content, at levels similar to those for the pre-industrial Holocene (Siegenthaler et al., 2005). In particular, it includes the MIS 11c, traditionally considered as potential analogue for future climate evolution because of relatively similar orbital climate forcing (Loutre and Berger 2000; Masson-Delmotte et al., 2006; Tzedakis et al., 2012). Therefore, a thorough study of this interval will provide information on type and magnitude of climate variability under non-anthropogenic but otherwise comparable conditions to the present.

In addition, the studied interval also includes the MIS 12, the most extreme glacial of the last 500 ka (Shackleton, 1987; Rohling et al., 1998; Lisiecki and Raymo, 2005) characterised by a sea level of about 125 m lower than today (Rohling et al. 2009; 2014). The MIS 12-11 transition (Termination

V) is also part of this peculiar interval. It represents a glacial-interglacial transition that is long compared to later Pleistocene terminations (Oppo et al., 1998; Bauch et al., 2000; Thunell et al., 2002; Kandiano and Bauch, 2007; Helmke et al., 2008).

Notwithstanding the huge literature about the aforementioned climatic intervals, some features deserve additional clarifications. Two of the most intriguing aspects are the protracted deglaciation during Termination V and the cause of a long period of interglacial warmth during the MIS 11 (longer than any other mid-to late Pleistocene interglacial) with contrasting SST dynamics between polar- and mid-latitudes (Helmke and Bauch, 2003; Kandiano and Bauck, 2007; Kandiano et al., 2012 Milker et al. 2013 and references therein).

These issues could be addressed by analysing paleo-data from the Mediterranean Sea, a region highly sensitive to atmospheric and climatic system modifications due to its intermediate latitudinal position, where Euro-Asian and North-African climate regimes strongly interact (Roether et al., 1996; Béthoux et al., 1999; Pinardi and Masetti 2000; Trigo et al., 2004; Lionello et al., 2006).

Moreover the Mediterranean climate is exposed to the South-Asian Monsoon in summer and the Siberian High-Pressure-System in winter (Luterbacher, 2005; Lionello et al., 2006). Today, the southern part of the Mediterranean region is mostly influenced by the descending branch of the Hadley cell, while the northern part is more linked to mid-latitude variability, characterized by the North-Atlantic Oscillation (NAO) and other mid-latitude teleconnection patterns (Hurrel et al., 2004). Thus, climate investigations of geological archives of the Mediterranean region reflect paleo-changes in the intensity and extension of global-scale climate patterns. In addition, the Mediterranean sedimentary sequences are characterized by the (quasi-) periodical occurrence of episodes of deep-sea oxygen depletion (sapropel layers) (Olausson, 1991; Rohling et al., 2015 and references therein). Based on their link with the astronomical parameters (Hilgen 1991; Rossignol–Strick, 1983; Lourens 2004; Konijnendijk et al., 2014) these discrete levels represent a useful constraint to establish accurate age models for marine and land sections.

We present a new high-resolution quantitative study of planktonic foraminifera distribution throughout MIS 13-9 for sediment core KC01B collected in the Ionian Sea, central Mediterranean Sea. Planktonic foraminifera are amongst the most commonly used proxies for paleoceanographic

and paleoclimate sea-surface reconstructions. Their distribution and abundance is strongly linked to surface-water properties. In addition, the physical and chemical properties of their shells reflect past environmental conditions of the water masses in which they lived (Kucera 2007 and references therein).

The investigated deep-marine sequence of core KC01B represents a key site for stratigraphic and paleoclimatic investigations. This is not only because of its strategic location but also because it was used for the construction of a sapropel-based astronomical timescale for the last 1.1 My (Lourens, 2004). Moreover, in this work, we update the studied time interval by using the recent chronological constraints on Pleistocene sapropel deposition (Konijnendijk et al. 2014) and a new oxygen isotopic record of *N. pachyderma*.

Our main aim is to explore how the ecosystem responded to climate variability during glacial and interglacial intervals throughout MIS 13–9 in order to discuss the possible mechanisms through which climate acts at the regional and global scale.

In detail, we focus on the main environmental and paleoceanographic processes occurring a) at times of glacial and interglacial MIS; b) during Termination V (T-V) and Termination IV (T-IV).

2. Modern Oceanographic Setting

Currently, the Mediterranean Sea is an evaporative basin where freshwater loss exceeds freshwater input, forcing an anti-estuarine circulation (Borghini et al., 2014).

At the surface (the first 100-200 m), moderate-salinity Atlantic Water (AW) intrudes through the Strait of Gibraltar and flows to the easternmost part of the Levantine basin modifying its temperature and salinity properties (Modified Atlantic Water – MAW). In the intermediate layer (depth between 150–200 and 600 m), Levantine Intermediate Water (LIW) forms in the eastern basin, spreads westwards and continues its flow towards the Strait of Gibraltar, and then into the Atlantic Ocean (Béthoux et al., 1992; Robinson et al., 1991; Manca et al., 2004; Malanotte-Rizzoli et al., 2014).

Atmospheric forcing and basin topography determine a large number of local cyclonic and anticyclonic cells (Pinardi and Masetti, 2000). In wintertime, outbreaks of cold and dry continental

air masses lead to significant negative heat budgets and buoyancy losses, initiating deep and/or intermediate dense water formation both in the western and in the eastern basins (Malanotte-Rizzoli and Bergamasco, 1991; Castellari et al., 2000).

The Ionian Sea is influenced by the transit and on-site transformation of the major water masses previously described (e.g., Modified Atlantic Water, MAW; Levantine Intermediate water, LIW; and Eastern Mediterranean Deep Water, EMDW, Malanotte-Rizzoli et al., 1997; Napolitano et al., 2000) (Fig. 1). At the near-surface level, most important for biological production, the MAW enters in the western Ionian basin advected by the Atlantic Ionian Stream (AIS) (Fig. 1). Recently, the upper-layer circulation in the Ionian Sea has been associated with the deep thermohaline circulation through the Bimodal Oscillating System (BiOS): the Ionian upper-layer circulation reverses from cyclonic to anticyclonic and vice versa on decadal time scale affecting the biological productivity in the northern Ionian and southern Adriatic Sea (Civitarese et al., 2010; Gačić et al., 2010).

The present-day Mediterranean Sea is characterized by oligotrophic conditions (Béthoux, 1979; Sarmiento et al., 1988). The main factor that controls the seasonal change in primary production is linked to the dynamics of the water column with increasing biomass in late winter/early spring and decreasing in summer (Antoine et al., 1995; Bosc et al., 2004; D'Ortenzio and Ribera d'Alcalà, 2009).

A significant West-East trophic gradient exists with nutrient depletion (mainly phosphorus) and a reduction in primary productivity in the eastern basin (Krom et al., 1991, 2010).

Moreover, primary productivity reflects the hydrological fragmentation due to mesoscale variability (D'Ortenzio and Ribera d'Alcalà, 2009).

An oligotrophic regime, characterized by a low production, occurs in summer, when a stable stratification takes place (Klein and Coste, 1984; Krom et al., 1992; Crispi et al., 1999; Allen et al., 2002). During this period, low standing stocks characterize surface waters with the dominance of predatory species. The Ionian planktonic foraminiferal association is generally dominated by *Globigerinoides ruber* pink (40-60%) and *G. ruber* alba (20-40%) with peaks of maximum abundance in the first 50 m of the water column (Pujol and Vergnaud Grazzini, 1995). Winter

convection, and less frequently frontal zone migration or upwelling, brings nutrients into the photic zone (mesotrophic regime) (Klein and Coste, 1984). During winter, the assemblage is characterized by the dominance of grazing species such as *Globorotalia truncatulinoides* (50%) and by the presence of other non-spinose species such as *Globorotalia inflata* (20%), and *Globigerina bulloides* (8%). *Globigerinoides ruber* alba (8%) and *Hastigerina siphonifera* (7%) are also part of the association. In detail, *G. inflata* and *G. ruber* alba are more abundant in the first 100 m of the water column, while *G. truncatulinoides* peaks at 200 meters water depth (Pujol and Vergnaud Grazzini, 1995).

The moderate mixing and ventilation processes, occurring during wintertime, bring the nutrients to the photic layer (Napolitano et al., 2000) as documented by the coccolithophorid occurrence in sediment traps collected in this area (Ziveri et al., 2000) and the satellite-derived surface chlorophyll concentration (D'Ortenzio and Ribera d'Alcalà, 2009). This hydrographic/oceanographic feature can also explain the presence of juvenile specimens of *G*. *inflata* and *G. truncatulinoides* in the surface layer (Pujol and Vergnaud Grazzini 1995).

3. Sediment core

Sediment core KC01B was collected from a small ridge on the lower slope of the southern Calabrian Ridge (Pisano Plateau, 36°15.250’ N, 17°44.340’ E, 3643 m water depth; Fig. 1) during cruise MD69 of the R/V Marion Dufresne in 1991.

The lithology consists of hemipelagic marls, with intercalation of sapropels and the presence of a number of thin tephra layers and few thin turbidite levels (Castradori 1993; Sanvoisin et al. 1993; Langereis et al. 1997; Lourens 2004).

This 37 m thick sediment sequence represents an invaluable opportunity of investigating the early to late Pleistocene. Core KC01B has been intensively studied from different points of view, i.e., planktonic foraminifera, nannoplankton, stable isotopes, chemical and paleomagnetic analyses, tephra and sapropel presence (Castradori 1993; Sanvoisin et al. 1993; Dekkers et al. 1994, van Santvoort et al. 1997; Langereis et al. 1997; Rossignol-Strick et al. 1998; Rossignol-Strick and Paterne, 1999; Lourens, 2004; Maiorano et al., 2013; Insinga et al., 2014).

Moreover, Core KC01B is well known in the chronostratigraphic literature because it was used for the construction of the Astronomical Time Scale (ATS) (Langereis et al., 1997) in the Mediterranean region and to propose the Tyrrhenian as a regional stage for the Upper Pleistocene (Cita et al., 2005). The ATS is based on the correlation of dominantly precession-controlled sedimentary cycles (*i.e*. sapropels and carbonate cycles) to astronomical parameters. In particular, this core was claimed to fill most of the gap between the oldest sapropel (S12) documented in marine sediments (piston core RC9-181 - eastern Mediterranean Sea) dated at 483 ka (Lourens et al., 1996a) and the youngest sapropel (v) exposed in the land-based marine successions of the Vrica section (Southern Italy) dated at 1.280 Ma (Lourens et al., 1996b).

Concomitantly, Rossignol-Strick et al. (1998) proposed an alternative independent age model based on tuning of the oxygen isotope record of KC01B with the ice sheet model of Imbrie and Imbrie (1980).

Differences between both age models are in the order of 0-5 kyr and result from the choice of two different target curves and the adopted time lags between insolation forcing and climate response (Langereis et al., 1997) (for discussion see Hilgen et al., 1993; Lourens et al., 1996a). Largest differences (in the order of 10 kyr) between both age models occur around 618 and 785 ka.

Subsequently, Lourens (2004) established an improved sapropel-tuned age model for this core based on high-resolution color reflectance correlation with the Ocean Drilling Project (ODP) Site 964. This time-scale resulted from a revised chronology of the marine isotope record of Rossignol-Strick et al. (1998), implying a much more uniform change in sedimentation rate for the Ionian Sea cores and a good fit with other Mediterranean and open ocean marine isotope records.

We studied the sediment interval through sections 21-16 of the core (between 21.82 and 15.85 m composite depth, spanning the time interval from 507.3 to 292.1 ka - Lourens, 2004). This interval includes three sapropels (S10, S11 and S12) (Lourens, 2004) (Fig. 2).

4. Methods

Quantitative micropaleontological analyses were performed on 596 samples with a spacing of 1 cm (average time resolution of ~ 380yr). Samples were washed through 63 micron sieves and oven

198 dried at 50°C. Planktonic foraminiferal assemblage composition was determined analysing the
199 >125 μm size fraction. For the micropaleontological census study, each sample was divided with a
200 microsplitter to obtain unbiased aliquots with more than 300 planktonic foraminifers per sample. All
201 taxa are quantified as percentages of the total number of planktonic foraminifers. The faunal data
202 sets described in this paper have been archived, and are available in digital form, at PANGEA.
203 In this study, *Globigerinoides sacculifer* includes *Globigerinoides trilobus*, *Globigerinoides*
204 *sacculifer* and *Globigerinoides quadrilobatus* (sensu Hemleben et al., 1989); *Neogloboquadrina*
205 *pachyderma* sinistral (sin) has been counted separately from the dextral (dex) form.
206 We distinguished *N. incompta* from *N. pachyderma* by its development of a distinct apertural rim
207 and a more lobulate outline. These taxa showed different vertical distribution and ecology. Studies
208 performed on living planktonic foraminifers in Japan seas and in the eastern North Atlantic
209 document the presence of *N. incompta* in shallower and warmer waters compared to *N.*
210 *pachyderma* (Kuroyanagi and Kawahata, 2004; Schiebel et al., 2001).
211 Moreover, different morphotypes of *Globigerinoides ruber* (white) were identified using the
212 morphotype concept of Wang (2000). The typical *Globigerinoides ruber* (d'Orbigny, 1839) is
213 reported as *G. ruber* sensu stricto (s.s.), whereas *Globigerinoides elongatus* (d'Orbigny, 1826) and
214 *Globigerinoides gomitulus* (Seguenza, 1880) are grouped and reported as *G. ruber* sensu lato
215 (s.l.).
216 Several investigations, based on molecular genetics and geochemistry, highlighted the need to
217 revise the taxonomy of *G. ruber* (d'Orbigny, 1839) which shows remarkable "morphological"
218 variations (inter alias Darling et al., 1999; Kuroyanagi et al. 2008). In addition, the discrimination of
219 the different morphotypes appears to be necessary because they have significantly different
220 habitat preferences and thus different stable isotopic signals (Wang, 2000; Kuroyanagi and
221 Kawahata, 2004; Loewemark et al., 2005; Kawahata, 2005; Lin and Hsieh, 2007; Numberger et al.,
222 2009). On the other hand, the recent investigation in the Gulf of Mexico of Thirumalai et al. (2014)
223 reports no evidence for discrepancies in s.s.-s.l. calcifying depth habitat or seasonality. The
224 controversial outcomes reported suggest that additional studies on the relationship between living
225 foraminiferal distribution and oceanographic conditions (productivity, stratification) in different

basins are necessary to build a more extensive picture of the ecological requirements of different foraminiferal genetic types. In this work, we distinguished between different morphotypes in order to test if they presented different distribution patterns in the past.

The paleoclimate curve was calculated following Cita et al. (1977) and Sanvoisin et al. (1993). It represents the algebraic sum of warm-water species percentages (expressed as positive values) and cold-water species percentages (expressed as negative values) based on ecological preferences and modern habitat characteristics reported in Hemleben et al. (1989), Rohling et al. (1993), and Pujol and Vergnaud-Grazzini (1995). Warm water species are all *G. ruber* (white and pink varieties), *G. sacculifer*, *Globigerinoides tenellus*, *Globigerina rubescens*, *Hastigerina siphonifera* (including *G. calida*) and *Orbulina universa*. The cold water species are *Globigerina bulloides*, *Globigerinita glutinata*, *Globorotalia scitula*, *Turbototalita quinqueloba* and *N. pachyderma* (dex). Negative and positive values of the curve allow qualitative estimates for cold and warm surface water respectively.

The paleoproductivity curve is based on a combination of planktonic foraminiferal species: it is calculated as the sum of *G. bulloides*, *G. glutinata* and *T. quinqueloba* percentages. All these taxa are related to high productivity environments (inter alias Bé and Tolderlund, 1971; Fairbanks and Wiebe, 1980; Pujol and Vergaud Grazzini, 1989).

In order to reconstruct paleoenvironmental and paleoceanographical conditions, the relative abundance of some species or groups considered in this study are plotted in percentages with respect to the total foraminiferal assemblage versus time. We assume that the habitat characteristics of the different species during the Pleistocene were similar to those observed today.

Stable isotope analyses were carried out on about 10-15 specimens of the planktonic foraminifers *N. pachyderma* (dex) and *G. ruber* (s.s. and s.l.) (from the >150 µm fraction) using an automated carbonate reaction device Kiel III coupled to a Thermo-Finnigan MAR253 Analytical precision was better than 0.03 and 0.05‰ for $\delta^{13}C$ and $\delta^{18}O$ respectively as deduced from international NBS-19, and in-house Naxos standards.

5. Age control

For the time interval considered in this work (290-510 ka), the age model by Lourens (2004) was partially modified and fine-tuned, considering the new chronological constraints on Pleistocene sapropel depositions (Konijnendijk et al. 2014).

We adopted the revised sapropel chronological framework in the eastern Mediterranean (ODP sites 967 and 968) provided by Konijnendijk et al. (2014) using the highly linear relation between the elemental ratio of titanium and aluminium in the sediment and insolation. The late Pleistocene sapropel chronology of Konijnendijk et al. (2014) presents deviation from Lourens (2004) down to ~400 ka, where sapropel S^b in ODP 967/968 (Emeis et al., 2000) is correlated to one insolation cycle older. Consequently, Sapropel S11 in KC01B [corresponding to sapropel S^b in ODP 967/968 (Konijnendijk et al., 2014)] does not correspond to insolation cycle 38 (as reported in Lourens, 2004 at 407 ka) but to cycle 40 with a corresponding age of 418.9 ka (Konijnendijk et al., 2014).

As additional constraint, we used the tuning of the new high-resolution $\delta^{18}O$ data from *N. pachyderma* (sin) with the open-ocean benthic oxygen isotopic stack from Lisiecki and Raymo (2005) (Fig. 2).

Interpolation between consecutive tie-points was carried out by a linear function, assuming a constant sedimentation rate between the consecutive tie-points (mean sedimentation rate of 0.035 m/ka) and resulted in a higher resolution age control than in previous investigations (Castradori 1993; Sanvoisin et al., 1993; Dekkers et al., 1994, van Santvoort et al., 1997; Langereis et al., 1997; Rossignol-Strick et al., 1998; Rossignol-Strick and Paterne, 1999). Data used for the age model construction are listed in table 1.

This new Mediterranean $\delta^{18}O$ stack of *N. pachyderma* (dex) in the core KC01B has been compared with the $\delta^{18}O$ data of *G. inflata* of Voelker et al. (2010) from the Atlantic Ocean and with the $\delta^{18}O$ records of *G. bulloides* from ODP-site 975 studied by Pierre et al. (1999) and modified by Lourens (2004) and Kandiano et al. (2012). The good visual comparison between these climatic records supports the adopted age model (Fig. 2).

6. Results

6.1 Foraminiferal assemblages

Foraminiferal assemblages are rich and well preserved. The Shannon-Weaver Index commonly varies between 0.99 and 2.6 (Fig. 3) and exhibits a sharply decreasing trend in diversity during the glacials MIS 12 and MIS 10. The more pronounced minima occur in the upper part of the glacial periods, when more than the 80% of the assemblages is composed by *T. quinqueloba*, neogloboquadrinids (*N. pachyderma* (dex) and *N. dutertrei*) and *G. bulloides* (Fig. 3). The remaining 20% of the assemblages is represented by *G. scitula* and *G. glutinata*. During the interglacials the diversity is higher with dominance of *G. ruber* group (about 50%) and the presence of other warm water taxa such as *O. universa*, *H. siphonifera*, *G.rubescens* and *G. tenellus* (10%). *G*. *bulloides*, neogloboquadrinids and T*. quinqueloba* show frequencies ranging from 10 to 20%.

The presence of *G. inflata* appears not to be related to glacial-interglacial phases; however higher abundances occur during interglacials (Fig. 3).

A discontinuous pattern is observed in the distribution of *G. sacculifer* and *Globorotalia truncatulinoides*. *G. sacculifer* peaks during interglacial phases with a maximum value of about 20% (Fig. 3). Its distribution is discontinuous during MIS 13, more continuous during MIS 11 and MIS 9. *G. truncatulinoides* characterises the foraminiferal assemblages during the middle and upper part of interglacials. The maximum abundance of this taxon (20-25%) is recorded during MIS 11 (Fig. 3).

7. Discussion

7.1 Glacials

Based on the planktonic foraminifera climatic curve, full glacial conditions occur during the upper part of MIS 12 and MIS 10 (Fig. 4). The climate conditions detected during the initial part of MIS 12 and MIS 10 are warmer than expected for a glacial stage as they fall in the range of values prevailing during the previously interglacials MIS 11 and MIS 9 (Fig. 4). These temperatures are principally related to higher percentages of warm surficial waters *G. ruber* group (Fig. 4). At this time, the assemblages are characterized by the dominance of *G. ruber* (s.l.) relative to *G*. *ruber*

(s.s.). All these morphotypes occur in tropical-subtropical regions and prefer well-stratified waters but they show different habitats and seasonal preferences. In general, *G. ruber* (s.l.) calcifies deeper than *G. ruber* (s.s.) (Wang, 2000; Lowermark et al., 2005) and reflects different nutrient availability due to stratification of the water column (Lin et al., 2004). Based on the ecological divergence of the morphotypes, we interpret the higher relative abundance of *G. ruber* (s.l.) during the early part of MIS 12 and 10 as indicative primarily of the deepening of the summer thermocline. Probably *G. ruber* (s.l.) has shifted their habitat in order to avoid oligotrophic surface waters documented at this time by the low values of the productivity curve (Fig. 4). In the present Mediterranean Sea, low levels of production occur in summer, when the summer thermocline deepens to ~90 m leading to a stable stratification (Klein and Coste, 1984; Krom et al., 1992). The small differences between $\delta^{18}O$ of *N. pachyderma* and *G. ruber* show that the two taxa share a similar habitat indicating more homogenous conditions during this interval between surface and intermediate waters (Fig. 4).

The climatic conditions detected during early MIS 12 in core KC01B are coeval with the relative wintertime warmer sea surface temperatures (SST) documented in the nearshore waters off Portugal and in the western Mediterranean basin by Voelker et al. (2010) and associated with the increased heat transport by the Azores Current across the Atlantic. Moreover, the warming detected during the lower half of MIS 10 displays the same warm temperature anomaly in the SST record of Site 980 (North Atlantic, Feni Drift) (McManus et al., 1999) and site 1089 (South Atlantic Subtropical Front) (Cortese et al., 2007) during full glacial MIS 10 centered at ca. 350 ka and linked by the authors to a stronger than usual Agulhas Current influence. These similarities can be explained by the quick response of sub-surficial Mediterranean waters to atmospheric processes during both glacial stages. The warming occurring during the glacial half of both glacial MIS 10 and MIS 12 implies an extra-regional connection between the Mediterranean sea and the northern and southern hemisphere.

The subsequent increase in abundances of cold-water indicators *T. quinqueloba*, *N. pachyderma* (dex) and *G. bulloides* document the establishment of full glacial conditions during MIS 12 and MIS 10 at about 455 ka and 360 ka, respectively (Fig. 4). Well-known environmental preferences of

these species for nutrient-rich environments (Be and Tolderlund, 1971; Fairbanks and Wiebe, 1980; Reynolds and Thunell, 1986; Pujol and Vergnaud-Grazzini, 1995; Sierro et al., 2003) suggest productive sea surface waters as also supported by the highest values of the paleoproductivity curve (Fig. 4). At this time the fertilization can be triggered by the concurrence of different factors. One is represented by eolian input due to enhanced North-African dust deposition in the eastern Mediterranean (Roberts et al., 2011) during the upper part of the last five glacial stages. However, eolian dust in general does not seem to provide an adequate and/or continuous source of nutrients to enhance primary production (Krom et al., 2005; Incarbona et al., 2008). Another important factor may be the higher buoyancy gradient due to the reduced Atlantic surface-waters inflow that has altered the equilibrium of vertical mixing in the water column.

The glacial sea-level lowstand at the time of MIS 12 and MIS 10, leads to a reduced Atlantic surface-water influx and thus to shoaling of the density gradient (pycnocline) between intermediate and surface waters within the Mediterranean. This shoaling is similar to what has been suggested for other glacial sea-level lowstands (Rohling and Gieskes, 1989; Rohling, 1991; Rohling and Bryden, 1994; Myers et al., 1998). This factor is more evident during MIS12 when sea level was about 125 m below present (Rohling et al., 2009) (Fig. 4). MIS 12 is generally dominated by higher abundances (compared to MIS 10) of *N. pachyderma* (dex) and *N. dutertrei* reaching up to 60% of the total assemblage. These taxa are indicative for the intensity of the deep chlorophyll maximum (DCM), occurring when the upper part of the water column is isothermal and cold (Rohling and Gieskes, 1989; Pujol and Vergnaud Grazzini, 1995). Such DCM may develop during periods of reduced deep mixing. Similar evidence comes from the offset observed between *N. pachyderma* and *G. ruber* oxygen isotope values (Fig. 4) that document stratification between the surficial and the lower part of the photic zone. This is consistent with a different density gradient in the water column due to the large decrease in Atlantic surface inflow.

The colder intervals of the investigated glacials are characterized by peaks in abundance of *N. pachyderma* (sin) (with values of 18%) at times of extremely negative, cold values of the climate curve (Fig. 5). *N. pachyderma* (sin) is known not only to prefer polar-subpolar waters (Hemleben et al., 1989; Bé and Tolderlund, 1971; Reynolds and Thunell, 1986; Dieckmann et al., 1991;

364 Johannessen et al., 1994), but also to be the dominant planktonic foraminiferal species during
365 Heinrich events recorded in the North Atlantic Ocean (Heinrich, 1988; Bond et al., 1992).
366 Very rare specimens of *N. pachyderma* (sin) have been towed at the end of summer in the Ionian
367 Sea (Pujol and Vergnaud-Grazzini, 1995); however this taxon is generally uncommon (<5%) in the
368 Mediterranean during the Quaternary (Thunell, 1978; Rohling and Gieskes, 1989; Rohling et al.,
369 1993; Hayes et al., 1999; Sprovieri et al., 2003; Hayes et al., 2005; Triantaphyllou et al., 2009;
370 Siani et al., 2010; Sprovieri et al., 2012). Significant percentages of *N. pachyderma* (sin) in the
371 western Mediterranean Sea during the last glacial period have been interpreted as the result of
372 polar water intrusions into the Mediterranean via the Strait of Gibraltar at the time of the Atlantic
373 Heinrich events (Cacho et al., 1999; Pérez-Folgado et al., 2003; Sierro et al., 2005). The increases
374 in the relative abundance of *N. pachyderma* (sin), coeval with a SST drop comparable for
375 distribution and amplitude to the Heinrich-type events, have also been documented during MIS5
376 (Combourieu Neobout et al., 2002; Martrat et al., 2004), throughout MIS 15-9 (Girone et al., 2013)
377 and during MIS 100 (Becker et al., 2006) in the western and eastern basin.
378 At the investigated site (Fig. 5), we observe that the distribution of *N. pachyderma* (sin) is positively
379 correlated with that of neogloboquadrinids and that, despite the different time-resolution of the
380 data, the significant increase in abundance of *N. pachyderma* (sin) correlates well with that
381 observed in the western Mediterranean (ODP Site 975) (Girone et al., 2013) and North Atlantic
382 Heinrich-type events (Stein et al., 2009; Rodrigues et al., 2011). In the Mediterranean Sea high
383 abundances of neogloboquadrinids are often associated with low-density water masses as
384 observed in sapropel deposition during colder climatic phases (Capotondi and Vigliotti, 1999; Negri
385 et al., 1999; Stefanelli et al., 2005). We can speculate that the cooling of Atlantic inflowing waters
386 due to iceberg melting, already documented in the western Mediterranean (Sierro et al., 2005;
387 Frigola et al., 2008), could also have affected the hydrological setting of the Ionian Sea. On the
388 other hand, this may have occurred because of the intense freshwater discharges into the
389 Mediterranean through the Black Sea from meltwater of lakes dammed by the Scandinavian ice
390 sheet (Sprovieri et al., 2012) and/or from NW African (Atlas) mountain glaciers (Rogerson et al.,
391 2008). At present, we do not have clear evidence for local sources of water; further high-resolution

392 studies are necessary to understand the occurrence and distribution of *N. pachyderma* (sin) in the
393 Mediterranean Sea.
394
395 7.2 Interglacials
396 From the paleoclimatic curve typical full interglacial conditions can for the first time be recognized
397 during MIS 11 at ~420 ka. The warm conditions culminate between 415 to 395 ka when the
398 microfauna is characterized by the presence of tropical-subtropical species *G. sacculifer* that
399 prefers warmer and shallower waters than *G. ruber* (Kuroyanagi and Kawahata, 2004). At present,
400 this species lives in the western Mediterranean at the end of summer (Pujol and Vergnaud-
401 Grazzini, 1995) and its distribution in surface sediments from west to east reflects its strong
402 temperature dependence (Thunel, 1978). The increase in abundance of *G. sacculifer* in the
403 Mediterranean has been reported to be associated to “Climatic Optima” during the late Holocene
404 intervals e.g. Medieval Warm Period, the Roman Age, the late Bronze Age and the Copper Age
405 (Piva et al., 2008; Lirer et al., 2013; 2014). According, we interpret the occurrence of this species in
406 core KC01B during interglacial MIS 11 and MIS 9 as indicative of the “Climatic Optimum
407 interval/Thermal maximum”. This interpretation concurs with the paleoclimate reconstruction of the
408 same period and for the same core, based on calcareous nannofossil assemblages (Maiorano et
409 al., 2013). The presence of an extended “Climatic Optimum”, lasting ~30 ka, has been documented
410 in SST records across the world ocean (McManus et al., 1999; Hodell et al., 2000; De Abreu et al.,
411 2005; Kandiano and Bauch, 2007; Dickson et al., 2009; Stein et al., 2009; Voelker et al., 2010),
412 from Antarctic ice cores (Petit et al., 1999; Jouzel et al., 2007) and in terrestrial pollen records
413 (Tzedakis, 2010). It occurs after a prolonged deglacial warming (Termination V) that extends into
414 MIS 11 with global and regional climate variability (Milker et al., 2013 and references therein).
415 The present high-resolution database provides new climatostratigraphic insights for the “Climatic
416 Optimum” of the central Mediterranean region. It is interesting to note that, during MIS 11, *G.*
417 *sacculifer* shows three different peaks of abundance concomitant with the decrease/absence of *G.*
418 *truncatulinoides* (Fig. 4). *G. sacculifer* reaches its maximum quantity in the Eastern Basin, where

surface waters remain relatively warm, and low nutrient contents prevail throughout the year due to the a relatively stable pycnocline at depth (Pujol and Vergnaud Grazzini, 1995).

Higher values of living *G. truncatulinoides* have been observed in the Mediterranean in areas of intense water mixing during winter, i.e. the North Western Basin (Pujol and Vergnaud Grazzini, 1995), while in the more stratified waters of the Eastern Basin it is rarely found (Core top database of Kallel et al. (1997).

Distributional trends of these taxa document that the "Climatic Optimum" of MIS 11 was not uniform but characterized by three distinct intervals with a year-around water column stratification and/or a weaker winter mixing with a consequent limited food supply. At the same time, higher values of the paleoclimate curve imply warmer superficial conditions or elevated winter sea surface temperatures (i.e. increase of the warm water taxa). The three warmer intervals present an estimated age of 415-410 ka, 408-403 ka, and 400-395 ka, respectively.

An interesting remark is that the peak from 400 to 395 ka is coeval with and shows the same length of the warm interval (400-395 ka Fig. 4) recorded in marine paleoclimate data off Iberia at the end of the MIS 11c (Koutsodendris and Zahn, 2014). Since that interval corresponds to an insolation minimum, this implies that orbital insolation forcing is not the warming cause.

Koutsodendris and Zahn (2014) motivate the North-Atlantic warmth as an interhemispheric teleconnection between strong leakage in the South Atlantic and Atlantic Meridional Overturning Circulation (AMOC)-driven warmth in the North Atlantic maintaining temperate conditions off Iberia and the continental Europe during the MIS11c. Accordingly, we speculate that the warmer intervals identified in our record are the result of an ocean-climate teleconnection between the high- and low- latitudes. Nevertheless additional sites are necessary in order to understand the exact mechanisms and extent of such climatic variability at time of the "Climatic Optimum".

The observed post-glacial temperature increase after Termination V does not match the Holocene SST trend when the "Climatic Optimum" already began after Termination I coincident with Sapropel S_1 deposition (Rohling and De Rijk, 1999; Capotondi et al., 1999; Cacho et al., 2001; Triantaphyllou et al., 2009). However a direct comparison between MIS 11 and MIS 1 is difficult to make because of a different phase in the orbital parameters. In fact, the present interglacial

447 (Holocene) spans a single summer insolation maximum (summer at 65ºN), while MIS 11
448 interglacial optimum spans two (weak) insolation maxima (Laskar et al., 2004).
449 From 392 ka onward, the MIS11 in core KC01B is characterized by oligotrophic surface waters
450 during summer (Fig. 4) and eutrophic during winter, when deep-water masses are well-ventilated,
451 as testified by the presence of *G. inflata* and *G. truncatulinoides*. These conditions are comparable
452 to those in the present-day Ionian Sea. At present, *G. inflata* and *G. truncatulinoides* dominate the
453 fauna of the winter assemblages in the Ionian Sea (Pujol and Verganud Grazzini, 1995).
454 Distribution of planktonic foraminifera during MIS 9 document similar general trends as described
455 for MIS 11, with a thermal maximum between 326 and 320 ka (Fig.4). However, MIS9 is
456 characterized by lower percentages of warm-water taxa compared to MIS 11, thus suggesting that
457 SSTs were lower during MIS9 than during MIS11.
458
459 7.3 Sea surface changes during transition T-V and T-IV
460
461 Termination V in core KC01B is marked by a decrease of $\delta^{18}O$ of *N. pachyderma* from +2.5‰ at
462 430 ka to +0.8‰ at 420 ka (Fig. 6). During this transition the planktonic foraminifera content shows
463 significant changes related to different environmental conditions (Fig. 6) and provides new data on
464 how the transitions evolved from glacial to interglacial.
465 The high abundance of the herbivorous species *G. bulloides* and *T. quinqueloba* from ~430 to
466 ~425 ka (Fig. 6) suggests enhanced nutrient supply in the sub-surface water masses. As these
467 species reach the highest concentrations in upwelling regions or in areas of vigorous vertical
468 mixing in the water column (Reynolds and Thunell, 1986), where high phytoplankton productivity
469 prevails, we can hypothesize the presence of an upwelling regime or continental coastal input at
470 this time, probably induced by the presence or intensification of the gyre similar to the one
471 observed at present in the Ionian Sea (Civitarese et al., 2010, Gacic et al., 2010). The absence of
472 *G. inflata* (Fig. 4) supports this oceanographic scenario, as this species prefers temperate and high
473 nutrient waters not affected by upwelling processes (Giraudeau 1993. The increase in primary
474 productivity is also documented by the calcareous nannofossil data (Maiorano et al., 2013). This
475 phase is coeval with a peak of iron-rich terrigenous dust at ODP Site 958 (Helmke et al., 2008),

related to the strengthening of trade winds over northwestern Africa. Probably, this strengthening of westerlies is also associated with the strengthening of the Atlantic Ionian Stream jet leading to a dynamic activity of mesoscale features such as meanders and eddies. The latter results in mixing thus in enhanced nutrient supply, and leads to increased primary production. Several oceanographic studies performed in different areas of the Mediterranean document that variability in mesoscale hydrographic features leads to an increase of biological productivity (Estrada, 1996; Christaki et al., 2011).

The relatively low abundance of *G. bulloides* between 424 and 420 ka, together with the increasing percentages of *N. pachyderma* (dex) and *N. dutertrei* (Fig. 6) documents the transition to stratified water conditions and the development of a DCM. The co-occurrence of *N. incompta, a species* that prefers shallower and warmer waters than *N. pachyderma* (Kuroyanagi and Kawahata, 2004), also suggests amelioration of climate (Fig. 6).

We interpret this microfaunal assemblage as the result of fresh-water input/land-derived nutrients associated with the climatic transition from glacial conditions of MIS 12 to the interglacial conditions of MIS 11. Further evidence is provided by the steadily decreasing $\delta^{18}O$ of *N. pachyderma* during the same period (Fig. 6), which might be explained by a SST increase or a salinity decrease due to surface water freshening during this phase.

The increase in *G. ruber* abundance at around 420 ka together with lighter oxygen isotopic values in *N. pachyderma* reflects the influence of the African humid phase in the Ionian sea that culminates with sapropel layer S11 deposition at 418.9 ka (Konijnendijk et al., 2014) (Fig. 6).

This is suggested by the timing that is coherent with the onset of the wet phase over North-West Africa (Helmeke et al., 2008), when the enhanced influence of the West African Monsoon system on the Saharan-Sahel region led to higher fresh-water input into the Mediterranean. During the early MIS 11 the African monsoon system intensification is also documented in marine records from the North Atlantic and western Mediterranean Sea and it has been related to the northward-moving of the Intertropical Convergence Zone (ITCZ) (Kandiano et al., 2012).

In general, changes in the planktonic foraminiferal distribution observed during transition T-IV lead to a similar climatic reconstruction as outlined for T-V (Fig. 6). The dominance of *G. bulloides* and

T. quinqueloba from 342 to 337 ka points to enhanced nutrient content and mixing/upwelling during the first part of the transition from MIS 10 to MIS9. The subsequent replacement (~ 336-333 ka) of *N. pachyderma* and *N. dutertrei* suggests stratified conditions with a shallow mixed layer. Then, Sapropel S10 occurs at 332 ka (Konijnendijk et al. 2014) (Fig. 6).

Based on our data, the dynamics of the sea surface property during Termination V are due to the deglaciation and wind system variability. The timing and modalities of climate dynamics during the Terminations in different regions are as yet not fully understood. Recent investigations focus on the relative position of the Heinrich cold events that characterize all last five Terminations at a global scale (Cortese et al., 2007; Cheng et al., 2009; Barker et al., 2011; Marino et al., 2015). During the most recent Terminations I (MIS 2/MIS 1) and II (MIS 6/MIS 5) their positions show strong differences in these two deglaciations and point to a bipolar seesaw control mechanism for Termination II (Marino et al., 2015).

Observing the distributional trend of *N. pachyderma* (sin) in core KC01B, a “Heinrich-like” cold event (see paragraph above) is clearly detected within both the transitions T-V and T-IV (Fig. 6) in correspondence with a small drop in the oxygen isotope record (Fig. 6). Based on paleoceanographic inferences provided by planktonic foraminifera, these cold episodes occur approximately in the mid-point of the deglaciations, coincident with the increase in trade wind intensity off NW Africa (Fig. 6). This suggests that they are probably linked to the wind influence and thus to atmospheric conditions. This interpretation is also consistent with reported results from other ocean basins, indicating that Heinrich-like events are associated with stronger winds (e.g. Wang et al., 2001; Moreno et al., 2002; Itambi et al., 2009; Roberts et al., 2011). These are probably induced by southward shifts of the Inter Tropical Convergence Zone (Jullien at al., 2007). Accordingly, we conclude that the T-V and T-IV observed in the Mediterranean are not only regional events but are associated with a dynamic reorganization of global atmospheric conditions.

Our environmental scenarios are consistent with the sequence of major events documented in the last four Terminations that link the displacements of the ITCZ, the AMOC and the North Atlantic cooling (Cheng et al., 2009; Schneider et al., 2014; Marino et al., 2015).

During glacial-interglacial transitions T-IV and T-V the climate/ocean interaction was probably related to strong feedback processes: the weakening or shutdown of the AMOC due to enhanced freshwater input to the North Atlantic resulted in an increase in sea surface temperature within the tropics as well as in cooling of the North Atlantic and in the geographical shift of the wind system over North Africa.

Clearly, more data with good age control are needed from a wider area so to substantiate and evaluate extent and intensity of these events. This is not only needed to better understand mechanisms of paleo-climate change but is also relevant for our abilities to forecast potential future climate change processes.

8. Conclusions

A detailed study on planktonic foraminiferal assemblages from sediment core (KC01B) collected in the Ionian Basin (central Mediterranean Sea) allowed us to reconstruct the climate variability during glacial- interglacial periods between 500 and 300 ka (MIS 13 - MIS9). The main results can be summarized as follows:

- The early part of MIS 12 and MIS 10 is characterized by relatively “warm conditions” with a deepening of the summer thermocline derived from the quantitative distribution of *G. ruber* s.l. with respect to *G. ruber* s.s. Glacial conditions and eutrophic regimes are established in the upper half of the interval evidenced by significant increase of *T. quinqueloba*, N. *pachyderma* (dex) and *G. bulloides*. The colder intervals are interrupted by peaks in abundance of *N*. *pachyderma* (sin) coeval with north-Atlantic Heinrich-type cold events suggesting the close association of Central Mediterranean climate and North-Atlantic millennial-scale climate instability.

- Interglacials MIS 11 and MIS 9 have a prolonged “Climatic Optimum” lasting ~20 and 6 Ka respectively, as documented by the increase of the warm species *G. sacculifer*. Here for the first time we document that the extended warmth during the MIS 11c is characterized by three intervals with elevated winter sea surface temperatures and a weaker winter mixing.

- Complex paleoceanographic changes occurred during the glacial - interglacial transitions (T-V and T-IV) consistent with the sequence of major events documented in the last four Terminations that link the displacements of the ITCZ, the AMOC and the North Atlantic cooling.

The high-resolution investigations allow us to provide the timing of these changes occurring in the Mediterranean region and to link these to global climate events.

Acknowledgements

The authors acknowledge L. van Roij, A. Filippidi, and A. van Dijk for isotope measurements. Special thanks go to two anonymous reviewers and the editor Paul Hesse for their helpful comments and suggestions. Discussions with E. Bonatti, L. Vigliotti and P. Montagna are gratefully acknowledged. This study was financially supported by NWO (PASSAP, PASS), EU-Mast (Paleoflux), NEXTDATA and RITMARE (Ricerca ITaliana per il MARE) projects. This is contribution number 1873 of the CNR-ISMAR of Bologna.

References

Allen, J.I., Somerfield, P.J., Siddorn, J., 2002. Primary and bacterial production in the Mediterranean Sea: a modelling study. Journal of Marine Systems 33-34, 473-495.

Antoine, D., Morel, A., André, J.M., 1995. Algal pigment distribution and primary production in the Eastern Mediterranean as derived from Coastal Zone Color Scanner observations. Journal of Geophysical Research, 100, 16193-16209.

Barker, S., Knorr, G., Edwards, R.L., Parrenin, F., Putnam, A.E., Skinner, L.C., Wolff, E., Ziegler, M., 2011. 800,000 Years of Abrupt Climate Variability. Science 347, 0-5.

Bauch, H.A., Erlenkeuser, H., Helmke, J.P., Struck, U., 2000. A paleoclimatic evaluation of marine oxygen isotope stage 11 in the high-northern Atlantic (Nordic seas). Global and Planetary Change 24, 27-39.

Bè, A.W.H., Tolderlund, D.S., 1971. Distribution and ecology of living planktonic foraminifera in surface waters of the Atlantic and Indian Oceans. In: Funnel, B.M., Riedel, W.R. (Eds.). The Micropaleontology of Oceans. Cambridge University Press, Cambridge, pp. 105-149.

Becker, J.F., Lourens, L.J., Raymo, M.E., 2006. High-frequency climate linkages between the North Atlantic and the Mediterranean during marine oxygen isotope stage 100 (MIS100). Paleoceanography 21, PA3002, http://dx.doi.org/ 10.1029/2005PA001168.

Béthoux, J.P., 1979. Budgets of the Mediterranean Sea. Their dependence on the local climate and on the characteristics of the Atlantic waters. Oceanologica Acta 2, 157-163.

590 Béthoux, J.P., Morin, P., Madec, C., Gentili, B., 1992. Phosphorus and nitrogen behaviour in the
591 Mediterranean Sea. Deep-Sea Research 39, 1641-1654.

592 Béthoux, J.P., Gentili, B., Morin, P., Nicolas, E., Pierre, C., Ruiz-Pino, D., 1999. The Mediterranean
593 Sea: a miniature ocean for climatic and environmental studies and a key for the climatic functioning
594 of the North Atlantic. Progress in Oceanography 44, 131-146.

595 Bond, G., Heinrich, H., Broecker, W., Labeyrie, L., McManus, J., Andrews, J., Huon, S., Jantschik,
596 R., Clasen, S., Simet, C., Tedesco, K., Klas, M., Bonani, G., Ivy, S., 1992. Evidence for massive
597 discharges of icebergs into the North Atlantic Ocean during the last glacial period. Nature 360,
598 245-249.

599 Borghini, M., Bryden, H., Schroeder, K., Sparnocchia, S., Vetrano, A., 2014. The Mediterranean is
600 becoming saltier. Ocean Science 10, 693–700.

601 Bosc, E., Bricaud, A., Antoine, D., 2004. Seasonal and interannual variability in algal biomass and
602 primary production in the Mediterranean Sea, as derived from 4 years of SeaWiFS observations,
603 Global Biogeochemical Cycles 18, GB1005.

604 Cacho, I., Grimalt, J., Pelejero, C., Canals, M., Sierro, F.J., Flores, J.A., Shackleton, N., 1999.
605 Dansgaard-Oeschger and Heinrich event imprints in Alboran Sea paleotemperatures,
606 Paleoceanography 14(6), 698–705.

607 Cacho, I., Grimalt, J.O., Canals, M., Sbaffi, L., Shackleton, N.J., Schònfeld, J., Zahn, R., 2001.
608 Variability of the western Mediterranean Sea surface temperatures during the last 25,000 years
609 and its connection with the northern hemisphere climatic changes. Paleoceanography 16, 40-52.

610 Capotondi, L., Borsetti, A.M., Morigi, C., 1999. Foraminiferal ecozones, a high resolution proxy for
611 the late Quaternary biochronology in the central Mediterranean Sea. Marine Geology 153, 253-
612 274.

613 Capotondi, L., Vigliotti, L., 1999. Magnetic and microfaunistical characterization of late Quaternary
614 sediments in the Western Mediterranean (ODP Leg 161). Inference on sapropel formation and
615 paleoceanographic evolution. In: Zahn, R., Comas, M.C., and Klaus, A. (Eds.) Proceedings of the
616 Ocean Drilling Program, Scientific Results, College Station TX, 161, 505-518.

617 Castellari, S., Pinardi, N., Leaman, K., 2000. Simulation of water mass formation processes in the
618 Mediterranean Sea: influence of the time frequency of the atmospheric forcing. Journal of
619 Geophysical Research 105, 24157-24181.

620 Castradori, D., 1993. Calcareous nannofossils and the origin of eastern Mediterranean sapropels.
621 Paleoceanography 8, 459-471.

622 Cheng, H., Edwards, R.L., Broecker, W.S., Denton, G.H., Kong, X., Wang, Y., Zhang, R., Wang X.,
623 2009. Ice age terminations. Science 326, 248–252.

624 Christaki, U., Van Wambeke, F., Lefevre, D., Lagaria, A., Prieur, L., Pujo-Pay, M., Grattepanche,
625 J.-D., Colombet, J., Psarra, S., Dolan, J.R., Sime-Ngando, T., Conan, P., Weinbauer, M.G.,
626 Moutin, T., 2011. The impact of anticyclonic mesoscale structures on microbial food webs in the
627 Mediterranean Sea. Biogeosciences Discuss 8, 185-220.

628 Cita, M.B., Vergnaud-Grazzini, C., Robert, C., Chamley, H., Ciaranfi, N., D' Onofrio, S., 1977.
629 Paleoclimatic record of a long deep-sea core from the eastern Mediterranean. Quaternary
630 Research 8, 205-235.

631 Cita Sironi, M.B., Capotondi, L., Asioli, A., 2005. The Tyrrhenian stage in the Mediterranean:
632 definition, usage and recognition in the deep-sea record. Rendiconti Accademia Lincei 9, 16, 297-
633 310.

634 Civitarese, G., Gačić, M., Lipizer, M., Eusebi Borzelli, G.L., 2010. On the impact of the Bimodal
635 Oscillating System (BiOS) on the biogeochemistry and biology of the Adriatic and Ionian Seas
636 (Eastern Mediterranean). Biogeosciences 7, 3987–3997.

637 Combourieu Nebout, N., Turon, J.L., Zahn, R., Capotondi, L., Londeix, L., Pahnke, K., 2002.
638 Enhanced aridity and atmospheric high-pressure stability over the western Mediterranean during
639 the North Atlantic cold events of the past 50 ky. Geology 30, 863–866.

640 Cortese, G., Abelmann, A., Gersonde, R., 2007. The last five glacial-interglacial transitions: A high-
641 resolution 450,000-year record from the subantarctic Atlantic. Paleoceanography 22 (4), PA4203.

642 Crispi, G., Crise, A., Mauri, E., 1999. A seasonal three-dimensional study of the nitrogen cycle in
643 the Mediterranean Sea: part II. Verification of the energy constrained trophic model. Journal of
644 Marine Systems 20, 357-380.

645 Darling, K.F., Wade, C.M., Kroon, D., Leigh Brown, A.J., Bijma, J., 1999. The diversity and
646 distribution of modern planktic foraminiferal small subunit ribosomal RNA genotypes and their
647 potential as tracers of present and past ocean circulations. Paleoceanography 14, 3-12.

648 De Abreu, L., Abrantes, F., Shackleton, N., Tzedakis, P.C., McManus, J.F., Oppo, D.W., Hall, M.A.,
649 2005. Ocean climate variability in the eastern North Atlantic during interglacial marine isotope
650 stage 11: a partial analogue for the Holocene? Paleoceanography 20, PA3009.
651 doi:10.1029/2004PA001091.

652 Dekkers, M.J., Langereis, C.G., Vriend, S.P., Van Santvoort, P.J.M., De Lange, G.J., 1994. Fuzzy
653 c-means cluster analysis of early diagenetic effects on natural remanent magnetisation acquisition
654 in a 1.1 Myr piston core from the central Mediterranean. Physics of the Earth and Planetary
655 Interiors 85, 155-171.

656 Dickson, A.J., Beer, C.J., Dempsey, C., Maslin, M.A., Bendle, J.A., McClymont, E.L., Pancost,
657 R.D., 2009. Oceanic forcing of the Marine Isotope Stage 11 interglacial. Nature Geoscience 2, 428-
658 433.

659 Dieckmann, G.S., Spindler, S., Lange, M.A., Ackley, S.F., Eicken, H., 1991. Antarctic sea ice: A
660 habitat for the foraminifer Neogloboquadrina pachyderma, Journal of Foraminiferal Research
661 21,181-194.

662 d'Orbigny, A.D., 1826. Tableau méthodique de la classe de céphalopodes. Annales Des Sciences
663 Naturelles 14, 1–277.

664 d'Orbigny A.D., 1839. Mollusques, echinodermes, foraminiferes et polypiers, recueillis aux illes
665 Canaries par Mm. Webb et Berthelot et décrits par Alcide D'Orbigny (2éme partie: Mollusques).
666 Paris: 117 pp.; 8 pls.

667 D'Ortenzio, F., Ribera d'Alcalà, M., 2009. On the trophic regimes of the Mediterranean Sea: a
668 satellite analysis. Biogeosciences 6, 139–148.

669 Emeis, K.C., Struck, U., Schulz, H.M., Rosenberg, M., Bernasconi, S.M., Erlenkeuser, H.,
670 Sakamoto, T., Martinez-Ruiz, F.C., 2000. Temperature and salinity variations of Mediterranean
671 Sea surface water over the last 16,000 years from records of planktonic stable oxygen isotopes
672 and alkenone unsaturation ratios. Palaeogeography, Palaeoclimatology, Palaeoecology158 (3-4),
673 259-280.

674 EPICA community members, 2004. Eight glacial cycles from an Antarctic ice core. Nature 429,
675 6992, 623-628.

676 Estrada, M., 1996. Primary production in the northwestern Mediterranean. Science Marine 60
677 (Suppl. 2), 55-64.

678 Fairbanks, R.G., Wiebe, P.H., 1980. Foraminifera and chlorophyll maximum: vertical distribution,
679 seasonal succession, and paleoceanographic significance. Science 209, 1524–1526.

680 Frigola, J., Moreno, A., Cacho, I., Canals, M., Sierro, F.J., Flores, J.A., Grimalt, J.O., 2008.
681 Evidence of abrupt changes in Western Mediterranean Deep Water circulation during the last 50
682 kyr: a high-resolution marine record from the Balearic Sea. Quaternary International 181, 88–104.

683 Gačić, M., Borzelli, G. L. E., Civitarese, G., Cardin, V., Yari, S., 2010. Can internal processes
684 sustain reversals of the ocean upper circulation? The Ionian Sea example. Geophysical Research
685 Letters *37* (9), 1-5.

686 Giraudeau, J., 1993. Planktonic foraminiferal assemblages in surface sediments from the
687 southwest African margin. Marine Geology 110, 47-62.

688 Girone, A., Capotondi, L., Ciaranfi, N., Di Leo, P., Lirer, F., Maiorano, P., Marino, M., Pelosi, N.,
689 Pulice, I., 2013. Paleoenvironmental changes at the lower Pleistocene Montalbano Jonico section
690 (southern Italy): Global versus regional signals. Palaeogeography, Palaeoclimatology,
691 Palaeoecology 371, 62–79.

692 Hayes A., Rohling E.J., De Rijk S., Kroon D., Zachariasse W.J., 1999. Mediterranean planktonic
693 foraminiferal faunas during the last glacial cycle. Marine Geology 153, 239–252.

694 Hayes, A., Kucera, M., Kallel, N., Sbaffi, L., Rohling, E.J., 2005. Glacial Mediterranean sea surface
695 temperature based on planktonic foraminiferal assemblages. Quaternary Science Review 24, 999-
696 1016.

697 Heinrich, H., 1988. Origin and consequences of cyclic ice rafting in the northeast Atlantic Ocean
698 during the past 130,000 years. Quaternary Research 29, 142–152.

699 Helmke J.P. and Bauch, H.A., 2003. Comparison of conditions between the polar and subpolar
700 North Atlantic region over the last five climate cycles. Paleoceanography 18, 2, 1036.

701 Helmke, J.P., Bauch, H. A., Röhl, U., Kandiano, E.S., 2008. Uniform climate development between
702 the subtropical and subpolar northeast Atlantic across marine isotope stage 11. Climate of the Past
703 4, 181-190.

704 Hemleben, C., Spindler, M., Anderson, O.R., 1989. Modern Planktonic Foraminifera. Springer,
705 New York, pp. 1-363.

706 Hilgen, F.J., 1991. Astronomical calibration of Gauss to Matuyama sapropels in the Mediterranean
707 and implication for the Geomagnetic Polarity Time Scale. Earth Planetary Science Letters 104,
708 226–244.

709 Hilgen, F.J., Lourens, L.J., Berger, A., Loutre, M.F., 1993. Evaluation of the astronomically
710 calibrated time scale for the late Pliocene and earliest Pleistocene. Paleoceanography 8, 549–
711 565.

712 Hodell, D.A., Charles, C.D., Ninneman, U.S., 2000. Comparison of interglacial stages in the South
713 Atlantic sector of the southern ocean for the past 450 ka: implications for marine isotope stage
714 (MIS) 11. Global and Planetary Change 24 (1), 7-26.

715 Hurrell, J.W., Hoerling, M.P., Phillips, A.S., Xu, T., 2004. Twentieth century North Atlantic climate
716 change. Part I: assessing determinism. Climate Dynamics 23, 371-389.

717 Imbrie, J., Imbrie, J. Z., 1980. Modeling the climatic response to orbital variations, Science, 207,
718 943– 953.

719 Incarbona, A., Di Stefano, E., Sprovieri, R., Bonomo, S., Censi, P., Dinarès-Turell, J., Spoto, S.,
720 2008. Variability in the vertical structure of the water column and paleoproductivity reconstruction in
721 the central-western Mediterranean during the Late Pleistocene. Marine Micropaleontology 69 (1),
722 26-41.

723 Insinga, D.D., Tamburrino, S., Lirer, F., Vezzoli, L., Barra, M., De Lange, G.J., Tiepolo M.,
724 Vallefuoco M., Mazzola, S., Sprovieri, M., 2014. Tephrochronology of the astronomically-tuned
725 KC01B deep-sea core, Ionian Sea: insights into the explosive activity of the Central Mediterranean
726 area during the last 200 ka. Quaternary Science Reviews 85, 63–84.

727 Itambi, A.C., von Dobeneck, T., Mulitza, S., Bickert, T. and Heslop, D., 2009. Millennial-scale
728 northwest African droughts related to Heinrich events and Dansgaard-Oeschger cycles: Evidence
729 in marine sediments from offshore Senegal. Paleoceanography 24: doi: 10.1029/2007PA001570.

730 Jansen, J.H.F., Kuijpers, A., Troelstra, S.R., 1986. A Mid- Brunhes climatic event: Long term
731 changes in global atmo- spheric and ocean circulation. Science 232, 619-622.

732 Johannessen, T., Jansen, E., Flatøy, A., Ravelo, A. C., 1994. The relationship between surface
733 water masses, oceanographic fronts and paleoclimatic proxies in surface sediments of the
734 Greenland, Iceland, Norwegian seas. In Carbon Cycling in the Glacial Ocean: Constraints on the
735 Ocean's Role in Global Change, NATO ASI Ser. I 117, Zahn, R. et al. (Eds), Springer, Berlin, pp.
736 61-86.

737 Jouzel, J., Masson-Delmotte, V., Cattani, O., Dreyfus, G., Falourd, S., Hoffmann, G., Minster, B.,
738 Nouet, J., Barnola, J.M., Chappellaz, J., Fischer, H., Gallet, J.C., Johnsen, S., Leuenberger, M.,
739 Loulergue, L., Luethi, D., Oerter, H., Parrenin, F., Raisbeck, G., Raynaud, D., Schilt, A.,
740 Schwander, J., Selmo, E., Souchez, R., Spahni, R., Stauffer, B., Steffensen, J.P., Stenni, B.,
741 Stocker, T.F., Tison, J.L., Werner, M., Wolff, E.W., 2007. Orbital and millennial Antarctic climate
742 variability over the past 800,000 years. Science 317, 793-796.

743 Jullien, E., Grousset, F., Malaizé, B., Duprat, J., Sanchez-Goni, M.F. Eynaud, F., Charlier, K.,
744 Schneider, R., Bory, A., Bout, V., Flores, J.A., 2007. Low-latitude "dusty events" vs. high-latitude
745 "icy Heinrich events". Quaternary Research 68, 3, 379-386.

Kallel, N., Paterne, M., Duplessy, J.C., Vergnaud-Grazzini, C., Pujol, C., Labeyrie, L., Arnold, M., Fontugne, M., Pierre, C., 1997. Enhanced rainfall in the Mediterranean region during the last sapropel event. Oceanologica Acta 20, 697– 712.

Kandiano, E.S., Bauch, H.A., 2007. Phase relationship and surface water mass change in the NorthEast Atlantic duringMarine Isotope stage 11 (MIS11). Quaternary Research 68, 445-455.

Kandiano, E.S., Bauch, H.a., Fahl, K., Helmke, J P., Röhl, U., Pérez-Folgado, M., Cacho, I., 2012. The meridional temperature gradient in the eastern North Atlantic during MIS11 and its link to the ocean–atmosphere system. Palaeogeography, Palaeoclimatology, Palaeoecology 333-334, 24-39..

Kawahata, H., 2005. Stable isotopic composition of two morphotypes of *Globigerinoides ruber* (white) in the subtropical gyre in the north Pacific. Paleontological Research 9 (1), 27-35.

Klein, P., Coste, P., 1984. Effects of wind stress variability on nutrient transport into the mixed layer. Deep-Sea Research 31, 21-37.

Konijnendijk, T.Y.M., Ziegler, M., Lourens, L.J., 2014. Chronological constraints on Pleistocene sapropel depositions from high-resolution geochemical records of ODP Sites 967 and 968. Newsletters on Stratigraphy 47 (3), 263-282.

Koutsodendris, A., Pross, J., Zahn, R., 2014. Exceptional Agulhas leakage prolonged interglacial warmth during MIS 11c in Europe. Paleoceanography 29, 1062-1071.

Krom, M.D., Kress, N., Brenner, S., Gordon, L.I., 1991. Phosphorus limitation of primary production in the eastern Mediterranean Sea. Limnology and Oceanography 36, 424-432.

Krom, M.D., Brenner, N.K., Neori, A., Gordon, L.I., 1992. Nutrient dynamics and new production in a warmcore eddy from the Eastern Mediterranean Sea. Deep-Sea Research 39, 467-480.

Krom, M.D., Thingstad, T.F., Brenner, S., Carbo, P., Drakopoulos, P., Fileman, T.W., Flaten, G.A.F., Groom, S., Herut, B., Kitidis, V., Kress, N., Law, C.S., Liddicoat, M.I., Mantoura, R.F.C., Pasternak, A., Pitta, P., Polychronaki, T., Psarra, S., Rassoulzadegan, F., Skjoldal, E.F., Spyres, G., Tanaka, T., Tselepides, A., Wassmann, P., Wexels Riser, C.,Woodward, E.M.S., Zodiatis, G., Zohary, T., 2005. Summary and overview of the CYCLOPS P addition Lagrangian experiment in the Eastern Mediterranean. Deep-Sea Research II 52, 3090–3108.

Krom, M.D., Emeis, K.C., Van Cappellen, P., 2010. Why is the Eastern Mediterranean phosphorus limited? Progress in Oceanography 85, 236–244.

Kucera, M., 2007. Planktonic foraminifera as tracers of past oceanic environments. In: Hillaire-Marcel, C. and de Vernal, A. (eds): Developments in Marine Geology, Volume 1, Proxies in late Cenozoic. Paleoceanography. Elsevier, ISBN 13: 9780444527554, pp. 213-262.

Kuroyanagi, A., Kawahata H., 2004. Vertical distribution of living planktonic foraminifera in the seas around Japan. Marine Micropaleontology 53, 173-196.

Kuroyanagi, A., Tsuchiya, M., Kawahata, H., Kitazato, H., 2008. The occurrence of two genotypes of the planktonic foraminifer *Globigerinoides ruber* (white) and paleoenvironmental implications. Marine Micropaleontology 68, 236-243.

Langereis, C.G., Dekkers, M.J., De Lange, G.J., Paterne, M., Van Santvoort, P. J. M., 1997. Magnetostratigraphy and astronomical calibration of the last 1.1 Myr from an eastern

785 Mediterranean piston core and dating of short events in the Brunhes. Geophysical Journal
786 International 129, 75-94.

787 Laskar, J., Robutel, P., Joutel, F., Gastineau, M., Correia, A.C.M., Levrard, B., 2004. A Long-term
788 Numerical Solution for the Insolation Quantities of the Earth: Astronomy and Astrophysics 428,
789 261- 285.
790
791 Lin, H.L., Wang, W.C., Hung, G.W., 2004. Seasonal variation of planktonic foraminiferal isotopic
792 composition from sediment traps in the South China Sea. Marine Micropaleontology 53 (3-4), 447–
793 460.

794 Lin, H.L., Hsieh, H.Y., 2007. Seasonal variations of modern planktonic foraminifera in the South
795 China Sea. Deep Sea Research Part II: Tropical Studies in Oceanography 54, 1634-1644.

796 Lionello, P., Malanotte-Rizzoli, P., Boscolo, R., Alpert, P., Artale, V., Li, L., Luterbacher, J., May,
797 W., Trigo, R., Tsimplis, M., Ulbrich, U., Xoplaki, E., 2006. The Mediterranean climate: an overview
798 of the main characteristics and issues. In: Lionello, P., Malanotte-Rizzoli, P., Boscolo, R. (Eds.),
799 Mediterranean Climate Variability. Elsevier, Amsterdam, The Netherlands, pp. 1-26.

800 Lirer, F., Sprovieri, M., Ferraro, L., Vallefuoco, M., Capotondi, L., Cascella, A., Petrosino, P.,
801 Insinga, D., Pelosi, N., Tamburrino, S., Lubritto, C., 2013. Integrated stratigraphy for the Late
802 Quaternary in the eastern Tyrrhenian Sea. Quaternary International 292, 71-85.

803 Lirer, F., Sprovieri, M., Vallefuoco, M., Ferraro, L., Pelosi, N., Giordano, L., Capotondi, L., 2014.
804 Planktonic foraminifera as bio-indicators for monitoring the climatic changes occurred during the
805 last 2000 years in the SE Tyrrhenian Sea. Integrative Zoology Journal 9, 542–554. Lisiecki, L.E.,
806 Raymo, M.E., 2005. A Pliocene–Pliestocene stack of 57 globally distributed benthic d18O records.
807 Paleoceanography 20, PA1003. doi:10.1029/2004PA001071.

808 Lisiecki, L.E., Raymo, M.E., 2005. A Pliocene–Pliestocene stack of 57 globally distributed benthic
809 d18O records. Paleoceanography 20, PA1003. doi:10.1029/2004PA001071.

810 Loewemark, L., Hong, W.L., Yui, T.F., Hung, G.W., 2005. A test of different factors influencing the
811 isotopic signal of planktonic foraminifera in surface sediments from the northern South China Sea.
812 Marine Micropaleontology 55/1–2, 49–62.

813 Lourens, L.J., Hilgen, F.J., Zachariasse, W.J., van Hoof, A.A.M., Antonarakou, A., Vergnaud-
814 Grazzini, C., 1996a. Evaluation of the plio-Pleistocene astronomical time scale. Paleoceanography
815 11, 391– 413.

816 Lourens, L.J., Hilgen, F.J., Raffi, I., Vergnaud-Grazzini, C., 1996b. Early Pleistocene chronology of
817 the Vrica section (Calabria, Italia). Paleoceanography 11, 797– 812.

818 Lourens, L.J., 2004. Revised tuning of Ocean Drilling Program Site 964 and KC01B
819 (Mediterranean) and implications for the d18O, tephra, calcareous nannofossil, and geomagnetic
820 reversal chronologies of the past 1.1 Myr. Paleoceanography 19, PA3010.

821 Loutre, M.F., 2003. Clues from MIS11 to predict the future climate - a modelling point of view.
822 Earth and Planetary Science Letters 212, 213-224.

823 Luterbacher, J., Xoplaki, E., 2005. 500-year winter temperature and precipitation variability over
824 the Mediterranean area and its connection to the large-scale atmospheric circulation. In: Bolle, H.-

825 J. (Eds.) Mediterranean Climate. Variability and Trends. Springer Verlag, Berlin, New York, pp.
826 133-153.

827 Maiorano, P., Tarantino, F., Marino, M., De Lange, G. J., 2013. Paleoenvironmental conditions at
828 Core KC01B (Ionian Sea) through MIS13–9: Evidence from calcareous nannofossil assemblages.
829 Quaternary International 288, 97-111.

830 Malanotte-Rizzoli, P., Bergamasco, A., 1991. The wind and thermally driven circulation of the
831 eastern Mediterranean Sea. Part II: The baro- clinic case. Dynamics of atmospheres and oceans
832 15, 355–419, doi:10.1016/0377-0265(91)90026-C.

833 Malanotte-Rizzoli, P., Artale, V., Borzelli-Eusebi, G.L., Brenner, S., Crise, A., Gacic, M., Kress N.,
834 Marullo, S., Ribera d'Alcalà, M., Sofianos, S., Tanhua, T., Theocharis, A., Alvarez, M., Ashkenazy,
835 Y., Bergamasco, A., Cardin, V., Carniel, S., Civitarese, G., D'Ortenzio, F., Font, J., Garcia-Ladona,
836 E., Garcia-Lafuente, J.M., Gogou, A., Gregoire, M., Hainbucher, D., Kontoyannis, H., Kovacevic,
837 V., E. Kraskapoulou, G. Kroskos, Incarbona, A., Mazzocchi, M.G., Orlic, M., Ozsoy E., Pascual, A.,
838 Poulain, P. M., Roether, W., Rubino, A., Schroeder, K., Siokou-Frangou, J., Souvermezoglou, E.,
839 Sprovieri, M., Tintoré, J., Triantafyllou, G., 2014. Physical forcing and physical/biochemical
840 variability of the Mediterranean Sea: a review of unresolved issues and directions for future
841 research. Ocean Science 10, 281–322.

842 Manca, B., Burca, M., Giorgetti, A., Coatanoan, C., Garcia, M.J., Iona, A. 2004. Physical and
843 biochemical averaged vertical profiles in the Mediterranean regions: an important tool to trace the
844 climatology of water masses and to validate incoming data from operational oceanography.
845 Journal of Marine Systems 48, 83-116.

846 Marino, G., Rohling, E.J., Rodrìguez-Sanz, L., Grant, K.M., Heslop, D., Roberts, A.P., Stanford,
847 J.D., Yu, J., 2015. Bipolar seesaw control on last interglacial sea level. Nature 522, 197.

848 Martrat, B., Grimalt, J.O., Lopez-Martinez, C., Cacho, I., Sierro, F.J., Flores, J.A., Zahn, R., Canals,
849 M., Curtis, J. H., Hodell, D.A., 2004. Abrupt temperature changes in the western Mediterranean
850 over the past 250,000 years. Science 306, 1762–1765.

851 Masson-Delmotte, V., Kageyama, M., Braconnot, P., Charbit, S., Krinner, G., Ritz, C., Guilyardi, E.,
852 Jouzel, J., Abe-Ouchi, A., Crucifix, M., Gladstone, R.M., Hewitt, C.D., Kitoh, A., LeGrande, A.N.,
853 Marti, O., Merkel, U., Motoi, T., Ohgaito, R., Otto-Bliesner, B., Peltier, W.R., Ross, I., Valdes, P.J.,
854 Vettoretti, G., Weber, S.L., Wolk, F., Yu, Y., 2006. Past and future polar amplification of climate
855 change: climate model intercomparisons and ice-core constraints. Climate Dynamics 26, 513-529.

856 McManus, J.F., Oppo, D.W., Cullen, J.L., 1999. A 0.5 million year record of millennial-scale climate
857 variability in the North Atlantic. Science 283, 971-974.

858 Milker, Y., Rachmayani, R., Weinkauf, M.F.G., Prange, M., Raitzsch, M., Schulz, M., Kucera, M.,
859 2013. Global and regional sea surface temperature trends during Marine Isotope Stage 11. Climate
860 of the Past 9, 2231- 2252.

861 Moreno, A., Cacho, I., Canals, M., Prins, M. A., Sánchez-Goñi, M. F., Grimalt, J. O., and Weltje, G.
862 J., 2002. Saharan dust transport and high latitude glacial climatic variability: the Alboran Sea
863 record. Quaternary Research 58, 318-328.

Myers, P.G., Haines, K., Rohling, E.J., 1998. Modelling the paleo-circulation of the Mediterranean: the last glacial maximum and the Holocene with emphasis on the formation of sapropel S1. Paleoceanography 13, 586-606.

Napolitano, E., Oguz, T., Malanotte-Rizzoli, P., Yilmaz, A., Sansone, E., 2000. Simulations of biological production in the Rhodes and Ionian basins of the eastern Mediterranean. Journal of Marine Systems 24, 277-298.

Negri, A., Capotondi, L., Keller, J., 1999. Calcareous nannofossils, planktonic foraminifera and oxygen isotopes in the late Quaternary sapropels of the Ionian Sea. Marine Geology, 157: 89-103.

Numberger, L., Hemleben, C., Hoffmann, R., Mackensen, A., Schulz, H., Wunderlich, J.-M., Kucera, M., 2009. Habitats, abundance patterns and isotopic signals of morphotypes of the planktonic foraminifer Globigerinoides ruber (d'Orbigny) in the eastern Mediterranean Sea since the Marine Isotopic Stage 12. Marine Micropaleontology 73 (1-2), 90-104.

Olausson, E., 1991. A post-Cromerian rise in sea level. In: Weller, G., Wilson, C.L., Severin, B.A.B. (Eds.), International Conference on the Role of Polar Regions in Global Change: Proceedings of a Conference Held Jun 11–15, 1990 at the University of Alaska Fairbanks vol. II. Geophysical Inst. Univ. of Alaska Fairbanks, pp. 496–498.

Oppo, D.W., McManus, J.F., Cullen, J.L., 1998. Abrupt climate events 500 000 to 340 000 years ago: evidence from subpolar North Atlantic sediments. Science 279, 1335-1338.

Perez-Folgado, M, Sierro, F.J., Flores, J.A., Cacho, I., Grimalt, J.O., Zahn, R., Shackleton, N.J., 2003. Western Mediterranean planktonic foramini- fera events and millennial climatic variability during the last 70kyr. Marine Micropaleontology 48, 49-70.

Petit, J.R., Jouzel, J., Raynaud, D., Barkov, N.I., Barnola, J.M., Basile, I., Bender, M., Chappellaz, J., Davis, J., Delaygue, G., Delmotte, M., Kotlyakov, V.M., Legrand, M., Lipenkov, V., Lorius, C., Pépin, L., Ritz, C., Saltzman, E., Stievenard, M., 1999. Climate and atmospheric history of the past 420,000 years from the Vostok Ice Core, Antarctica. Nature 399, 429-436.

Pierre, C., Belanger, P., Saliège, J.F., Urrutiaguer, M. J., Murat, A., 1999. Paleoceanography of the western Mediterranean during the Pleistocene: Oxygen and carbon isotope records at Site 975, Proceedings of the Ocean Drilling Program, Scientific Results 161, 481–488.

Pinardi, N., Masetti, E., 2000. Variability of the large-scale general circulation of the Mediterranean Sea from observations and mod- elling: a review. Palaeogeography Palaeoclimatology Palaeoecology 158, 153-173.

Piva, A., Asioli, A., Trincardi, F., Schneider, R. R., Vigliotti, L., 2008. Late-Holocene climate variability in the Adriatic Sea (Central Mediterranean). The Holocene 18 (1), 153-167.

Pujol, C., Vergnaud-Grazzini, C., 1989. Palaeoceanography of the last deglaciation in the Alboran Sea (western Mediterra- nean): Stable isotopes and planktonic foraminiferal records. Marine Micropaleontology 15, 153-179.

Pujol, C., Vergnaud-Grazzini, C., 1995. Distribution patterns of live planktonic foraminuifers as related to regional hydrography and productive system of the Mediterranean Sea. Marine Micropaleontology 25, 187-217.

Reynolds, l.A., Thunell, R.C., 1986. Seasonal production and morphologic variation of Neogloboquadrina pachyderma (Ehrenberg) in the northeast Pacific: Micropaleontology 32, 1–18.

Roberts, A. P., Rohling E. J,. Grant, K. M.,. Larrasoaña, J. C., Liu, Q., 2011. Atmospheric dust variability from Arabia and China over the last 500,000 years. Quaternary Science Reviews, 30, 3537-3541.

Robinson, A.R., Golnaraghi, M., Leslie, W.G., Artegiani, A., Hecht, A., Lazzoni, E., Michelato, A., Sansone, E.A., Theocharis, A., Unluata, U., 1991. Structure and variability of the Eastern Mediterranean general circulation. Dynamics of Atmospheres and Oceans 15, 215-240.

Rodrigues, T., Voelker, A.H.L., Grimalt, J.O., Abrantes, F., Naughton, F., 2011. Iberian Margin sea surface temperature during MIS15 to 9 (580–300 ka): glacial suborbital variability versus interglacial stability. Paleoceanography 26, PA1204, doi.:10.1029/2010PA001927.

Roether, W.H., Manca, B.B., Klein, B., Bregant, D., Georgopoulos, D., Beitzel, V., Kovacevic, V., Luchetta, A., 1996. Recent changes in eastern Mediterranean deep waters. Science 271, 333-335.

Rogerson, M., Cacho, I., Jimenez-Espejo, F., Reguera, M.I., Sierro, F.J., Martinez-Ruiz, F., Frigola, J., Canals, M., 2008. A dynamic explanation for the origin of the western Mediterranean organic-rich layers. Geochemistry, Geophysics, Geosystems 9, Q07U01. doi:10.1029/2007GC001936.

Rohling, E.J., Gieskes, W.W.C., 1989. Late Quaternary changes in Mediterranean intermediate water density and formation rate. Paleoceanography 4, 531–545.

Rohling, E.J., 1991. A simple two-layered model for shoaling of the eastern Mediterranean pycnocline due to glacio-eustatic sea level lowering. Paleoceanography 6, 537–541.

Rohling, E.J., Jorissen, F.J., Vergnaud-Grazzini, C., Zachariasse, W.J., 1993. Northern Levantine and Adriatic Quaternary planktic foraminifera; Reconstruction of paleoenvironmental gradients. Marine Micropaleontology 21, 191-218.

Rohling, E.J., 1994. Review and new aspects concerning the formation of eastern Mediterranean sapropels. Marine Geology 122, 1-28.

Rohling, E.J., Fenton, M., Jorissen, F.J., Bertrandt, P., Gans- sen, G., Caulet, J.P., 1998. Magnitudes of sea-level low- stands of the past 500,000 years. Nature 394, 162-164.

Rohling, E.J., De Rijk, S., 1999. The Holocene Climate Optimum and Last Glacial Maximum in the Mediterranean: The marine oxygen isotope record. Marine Geology 153, 57-75.

Rohling, E.J., Grant, K., Bolshaw, M., Roberts, A.P., Siddall, M., Hemleben, Ch, Kucera, M., 2009. Antarctic temperature and global sea level closely coupled over the past five glacial cycles. Nature Geoscience 2, 500-504.

Rohling, E.J., Foster, G.L., Grant, K.M., Marino, G., Roberts, A.P., Tamisiea, M.E., Williams, F., 2014. Sea-level and deep-sea-temperature variability over the past 5.3 million years. Nature 508, 477–482.

Rohling, E. J., Marino, G., Grant, K. M., 2015. Mediterranean climate and oceanography, and the periodic development of anoxic events (sapropels). Earth-Science Reviews 143, 62–97.

940 Rossignol-Strick, M., 1983. African monsoons, an immediate climate response to orbital insolation.
941 Nature 30, 446–449.

942 Rossignol-Strick, M., Paterne, M., Bassinot,F., Emeis,K.-C., DeLange,G.J., 1998. An unusual mid-
943 Pleistocene monsoon period over Africa and Asia. Nature 392, 269-272.

944 Rossignol-Strick, M., Paterne M., 1999. A synthetic pollen record of the eastern Mediterranean
945 sapropels of the last 1 Ma: Implications for the time-scale and formation of sapropels. Marine
946 Geology 153, 221–237.

947 Sanvoisin, R., D'Onofrio, S., Lucchi, R., Violanti, D., Castradori, D., 1993. 1 Ma Paleoclimatic
948 record from the Eastern Mediterranean Marflux Project: the first results of micropaleontological and
949 sedimentological investigation of a long piston core from the Calabrian Ridge. Il Quaternario 6,
950 169–188.

951 Sarmiento, J., Herbert, T., Toggweiler, J.R., 1988. Mediterranean nutrient balance and episodes of
952 anoxia. Global Biogeochemical Cycles 2, 427-444.

953 Schiebel, R., Waniek, J.J., Matthias, B., Hemleben, C., 2001. Planktic foraminiferal production
954 stimulated by chlorophyll redistribution and entrainment of nutrients. Deep Sea Research Part I.
955 Oceanographic Research Papers 48 (3), 721-740.

956 Schneider, T., Bischoff, T., Haug, G.H., 2014. Migrations and dynamics of the intertropical
957 convergence zone. Nature 513, 45–53.

958 Seguenza, G., 1880. Le formazioni terziarie nella provincia di Reggio (Calabria): Rendiconti
959 Accademia dei Lincei, CI. Sci. Fis. Mat. Nat., Mem., ser. 3, v.6, 3-446, tav. 1-17.

960 Shackleton, N.J., 1987. Oxygen isotopes, ice volume and sea level. Quat. Sci. Rev. 6, 183-190.

961 Siani, G., Paterne, M., Colin, C., 2010. Late Glacial to Holocene planktonic foraminifera bioevents
962 and climatic record in the South Adriatic Sea, Journal of Quaternary Science 25, 808–821.

963 Siegenthaler U., Stocker T.F., Monnin E., Luethi D., Schwander J., Stauffer B., Raynaud D., et al.,
964 2005. Stable carbon cycle-climate relationship during the late Pleistocene. Science 310, 1313-
965 1317.

966 Sierro F.J., Flores, J.A., Frances,G., Vazquez, A., Utrilla, R., Zamarreno, I., Erlenkeuser, H.,.
967 Barcena, M.A., 2003. Orbitally-controlled oscillations in planktic communities and cyclic changes in
968 western Mediterranean hydrography during the Messinian. Palaeogeography, Palaeoclimatology,
969 Palaeoecology 190, 289-316.

970 Sierro, F.J., Hodell, D.A., Curtis, J.H., Flores, J.A., Reguera, I., Colmenero-Hidalgo, E., Bárcena,
971 M.A., Grimalt, J.O., Cacho, I., Frigola, J., Canals, M., 2005. Impact of iceberg melting on
972 Mediterranean thermohaline circulation during Heinrich events. Paleoceanography 20, PA2019,
973 doi:10.1029/2004PA001051.

974 Sprovieri, R., Di Stefano, E., Incarbona, A., Gargano, M.E., 2003. A high- resolution record of the
975 last deglaciation in the Sicily Channel based on foraminifera and calcareous nannofossil
976 quantitative distri-bution. Palaeogeography, Palaeoclimatology, Palaeoecology 202, 119–142.

977 Sprovieri, M., Di Stefano, E., Incarbona, A., Salvagio Manta, D., Pelosi, N., Ribera d'Alcalà, M.,
978 Sprovieri, R., 2012. Centennial to millennial scale climate oscillations in the Central Eastern
979 Mediterranean Sea between 20,000 and 70,000 years ago: evidence from a high-resolution
980 geochemical and micropaleontological record. Quaternary Science Reviews 46, 126-135.

981 Stefanelli, S., Capotondi, L., Ciaranfi, N., 2005. Foraminiferal record and environmental changes
982 during the deposition of the early- middle Pleistocene sapropels in southern Italy.
983 Palaeogeography, Palaeoclimatology, Palaeoecology 216, 27–52.

984 Stein, R., Hefter, J., Grützner, J., Voelker, A., Naafs, B.D.A., 2009. Variability of surface water
985 characteristics and Heinrich-like events in the Pleistocene midlatitude North Atlantic Ocean:
986 biomarker and XRD records from IODP Site U1313 (MIS16-9). Paleoceanography 24,
987 doi:10.1029/2008PA001639.

988 Thirumalai, K., Richey, J.N., Quinn, T.M., Poore, R.Z., 2014. Globigerinoides ruber morphotypes in
989 the Gulf of Mexico: A test of null hypothesis. Scientific Reports 4, 6018.

990 Thunell, R.C., 1978. Distribution of recent planktonic foraminifera in surface sediments of the
991 Mediterranean Sea. Marine Micropaleontology 3, 147–173.

992 Thunell, R.C., Poli, M-S., Rio, D., 2002. Changes in deep and intermediate water properties in the
993 western North Atlantic during marine isotope stages 11–12: evidence from ODP Leg 172, Marine
994 Geology 189, 63–77.

995 Triantaphyllou, M.V., Ziveri, P., Gogou, A., Marino, G., Lykousis, V., Bouloubassi, I., Emeis, K.C.,
996 Kouli, K., Dimizia, M., Rosell-Mele, A., Papanikolaou, M., Katsouras, G., Nunez, N., 2009. Late
997 GlacialeHolocene climate variability at the south-eastern margin of the Aegean Sea. Marine
998 Geology 266, 182-197.

999 Trigo, R.M., Pozo-Vazquez, D., Osborn, T.J., Castro-Dıez, Y., Gamiz-Fortis, S., Esteban-Parra,
1000 M.J., 2004. North Atlantic oscillation influence on precipitation, river flow and water resources in
1001 the Iberian Peninsula. International Journal of Climatology 24, 925-944.

1002 Tzedakis, P.C., 2010. The MIS 11—MIS 1 analogy, southern European vegetation, atmospheric
1003 methane and the early anthropogenic hypothesis. Climate of the Past 6, 131–144.

1004 Tzedakis, P.C., Channell, J.E.T., Hodell, D.A., Kleiven, H.F., and Skinner, L.C., 2012a.
1005 Determining the natural length of the current interglacial. Nature Geoscience 5, 138–141.
1006

1007 van Santvoort, P. J.M., De Lange, G.J., Langereis, C.G., Dekkers, M.J., 1997. Geochemical and
1008 paleomagnetic evidence for the occurrence of ''missing'' sapropels in eastern Mediterranean
1009 sediments, Paleoceanography 12 (6), 773-786.

1010 Voelker, A.H.L., Rodrigues, T., Hefter, J., Billups, K., Oppo, D., McManus, J., Stein, R., Grimalt,
1011 J.O., 2010. Variations in mid-latitude North Atlantic surface water properties during the mid-
1012 Brunhes (MIS9–14) and their implications for the thermohaline circulation. Climate of the Past 6,
1013 531-552.

1014 Wang, L.J., 2000. Isotopic signals in two morphotypes of *Globigerinoides ruber* (white) from the
1015 South China Sea: implications for monsoon climate change during the last glacial cycle.
1016 Palaeogeography, Palaeoclimatology, Palaeoecology 161 (3–4), 381–394.

1017 Wang, Y.J., Cheng, H., Edwards, R.L., An, Z.S., Wu, J.Y., Shen, C.C., Dorale J.A., 2001. A high-
1018 resolution absolute-dated late Pleistocene monsoon record from Hulu Cave, China. Science 294,
1019 2236–2239.

1020 Ziveri, P., Rutten, A., de Lange, G.J., Thomson, J., Corselli, C., 2000. Present-day coccolith fluxes
1021 recorded in central Eastern Mediterranean sediment traps and surface sediments.
1022 Palaeogeography, Palaeoclimatology, Palaeoecology 158, 175-195.

Figure captions

Fig. 1. (a) Location map of the investigated core site KC 01B and the discussed references cores; (b) Bathymetric map of the Ionian Sea (DTM 450 m resolution retrieved from http://portal.emodnet-hydrography.eu/EmodnetPortal/index.jsf#); (c) mesoscale surface water circulation features of the Ionian Sea (from Napolitano et al. 2000 modified) are indicated (AIS= Atlantic-Ionian Stream, MAW= Modified Atlantic Water, MIJ= Mid Ionian Jet).

Fig. 2 - Comparison in time domain between the benthic oxygen isotopic stack of Liesicki and Raymo, (2005), the δ18O *G. inflata* record of Voelker et al. (2010), the δ18O *G. bulloides* record of Pierre et al. (1999) modified by Lourens (2004) and Kandiano et al. (2012), the δ18O *Globigerinoides ruber* and *Neogloboquadrina pachyderma* dex records from the study KC01B core [3 points moving average (thick black curve) are superimposed on the δ18O raw data], and the astronomical insolation curve of Laskar et al. (2004).

Fig 3 (a) Lithological log of sedimentary investigated time interval of core KC 01B, (b) planktonic oxygen isotope records, (c) diversity and (d) foraminiferal distribution (in percentages of total assemblages *versus age*) of the identified species. As “other” we grouped taxa with percentages <0.5 %. Chronology of sapropel (S10-S12) are according to Konijnendijk et al. (2014).

Fig. 4 Quantitative distribution patterns of selected planktonic species (percentage values plotted *versus age*) during MIS 13 and MIS 9 from core KC01B. Curve of Summer insolation at 65°N is from Laskar et al. (2004). Relative sea level record is from Rohling et al. (2009). Grey bands indicate interglacial intervals according to oxygen isotope chronology of Lisiecki and Raymo (2005); yellow bands correspond to the climatic optimum intervals. The MIS 13-9 and Termination V (T-V) and IV (T-IV) are indicated.

Fig. 5. Comparison between *N. pachyderma* (dex) δ18O, foraminiferal paleoclimate curve; neogloboquadrinids and relative abundance of *N. pachyderma* (sin) records at core site KC01B and foraminiferal SST (f) and plot of *N. pachyderma* (sin.) at Mediterranean ODP Site 975 (Girone et al., 2013). For the Atlantic climate records are indicated: Alkenone-based SST and relative proportion of ice ice-rafted detritus (IRD) at Core MD03-2699 (Rodrigues et al., 2011). *N. pachyderma* (sin) distribution record and (m) proportion of IRD at core MD 01-2446 (Marino et al., 2014 and Voelker et al., 2010), the dolomite relative intensity at IODP Site U1313 (Stein et al., 2009). Light blu bands mark abrupt fluctuations of *N. pachyderma* (sin.) correlated to Heinrich-type events recorded at the western Mediterranean and Atlantic sites.

Fig. 6. Down core distribution of selected planktonic species during Termination V and IV from core KC01B. Curve of Summer insolation at 65°N is from Laskar et al. (2004). The colour bands indicate the different phases (see text for the descriptions). Position of sapropel S10 and S11 and Termination V (T-V) and IV (T-IV) are indicated. H1 and H4 refer to Heinrich-like event 1 and 4 following the nomenclature adopted by Girone et al. (2013).

Central Mediterranean Mid-Pleistocene paleoclimatic variability and its association with global climate

Lucilla Capotondi[1*], Angela Girone[2], Fabrizio Lirer [3], Caterina Bergami[1,4], Marina Verducci[5], Mattia Vallefuoco[3], Angelica Afferri[2], Luciana Ferraro[3], Nicola Pelosi[3], Gert J. De Lange[6]

1) CNR - Istituto Scienze Marine (ISMAR)- ~~CNR,~~ Via Gobetti 101 40129 Bologna, Italia

2) Dipartimento di Scienze della Terra e Geoambientali, Università di Bari Aldo Moro

3) CNR - Istituto per l'Ambiente Marino Costiero (IAMC) - ~~CNR,~~ Calata Porta di Massa, Interno Porto di Napoli, 80133, Napoli, Italia

4) CNR - ~~National Research Council of Italy, IBAF -~~ Institute of Agro-environmental and Forest Biology ~~in Montelibretti,~~(IBAF) Italy

5) Dipartimento di Scienze della Terra, Università di Siena, Italia

6) Department of Earth Sciences - Geochemistry, Faculty of Geosciences, Utrecht University

* corresponding author: lucilla.capotondi@bo.ismar.cnr.it

Keywords: Planktonic foraminifera, Middle Pleistocene, Central Mediterranean, Paleoceanographic changes.

Abstract

Planktonic foraminiferal assemblages were studied at high-resolution in core KC–01B from the Ionian Sea. Quantitative analysis allowed us to distinguish the main climatic features and associated paleoceanographic changes, that occurred between Marine Isotopic Stages (MIS) 13 and 9 (~ 500-~~-~~300 ka).

MIS 12 and MIS 10 are characterized by relatively temperate conditions and an oligotrophic oceanographic regime in the early part and by colder conditions and nutrient supply in the sub-surface water masses in the upper part. During these intervals, small but distinct peaks of *Neogloboquadrina pachyderma* sinistral (sin) are detected at times of extremely negative values of

the planktonic foraminifera paleoclimatic curve. Their co-occurrence with similar episodes in the Atlantic suggests that the climate in the Central Mediterranean was associated with north-Atlantic millennial-scale climate instability. MIS 11 and MIS 9 are dominated by surficial warm-water taxa. The climate optimum is reached in the middle part of each of these stages, as denoted by the presence of *Globigerinoides sacculifer*, and persists for approximately 20 and 6 ka during MIS 11 and MIS 9 respectively. This warming ~~was~~ is not constant but is characterized by three distinct intervals with elevated winter temperatures and/or weak winter mixing.

Distribution of *Globigerina bulloides*, *Turborotalita quinqueloba* and *Neogloboquadrina pachyderma* dextral (dex) indicates that significant environmental changes occur across the transitions from glacial to interglacial MIS 12/MIS 11 (Termination V) and MIS 10/MIS 9 (Termination IV).

The studied record documents a close linkage between Mediterranean climate evolution and higher- and lower-latitude climate change throughout MIS 13—9.

1. Introduction

To improve our understanding of natural climate variability and our abilities to forecast future climate change, it is essential to investigate geological climate archives with relevant climate change events. Accordingly, this paper focuses on climate variability that occurred before and after the Mid-Brunhes event (MBE) (Jansen et al., 1986) in the Mediterranean Sea. The investigated time interval (MIS 13-MIS 11; ~ 500-300 ka) ~~was~~ is characterized by substantially warmer interglacials, (Epica Members, 2004; Jouzel et al., 2007) and ~~an increase in~~enhanced atmospheric CO_2 content, at levels similar to those for the pre-industrial Holocene (Siegenthaler et al., 2005). In particular, it includes the MIS 11c, traditionally considered as potential analogue for future climate evolution because of relatively similar orbital climate forcing (Loutre and Berger 2000; Masson-Delmotte et al., 2006; Tzedakis et al., 2012). Therefore, a thorough study of this interval will provide information on type and magnitude of climate variability under non-anthropogenic but otherwise comparable conditions to the ~~present conditions~~present ~~conditions~~.

In addition, the studied interval also includes the MIS 12, the most extreme glacial of the last 500 ka (Shackleton, 1987; Rohling et al., 1998; Lisiecki and Raymo, 2005) characterised by a sea level

of about 125 m lower than ~~today~~ today (Rohling et al. 2009; 2014). The MIS 12-~~-~~11 transition (Termination V) is also part of this peculiar interval. It represents a glacial-interglacial transition that is long compared to later Pleistocene terminations (Oppo et al., 1998; Bauch et al., 2000; Thunell et al., 2002; Kandiano and Bauch, 2007; Helmke et al., 2008).

Notwithstanding the huge literature about the aforementioned climatic intervals, some features deserve additional clarifications. Two of the most intriguing aspects are the protracted deglaciation during Termination V and the cause of a long period of interglacial warmth during the MIS 11 (longer than any other mid-to late Pleistocene interglacial) with contrasting SST dynamics between polar- and mid- latitudes (Helmke and Bauch, 2003; Kandiano and Bauck, 2007; Kandiano et al., 2012 Milker et al. 2013 and references therein).

These issues could be addressed by analysing paleo-data from the Mediterranean Sea, a region highly sensitive to atmospheric and climatic system modifications due to its intermediate latitudinal position, where Euro-Asian and North-~~african~~African climate regimes strongly interact (Roether et al., 1996; ~~Bethoux~~ Béthoux et al., 1999; Pinardi and Masetti 2000; Trigo et al., 2004; Lionello et al., 2006).

Moreover the Mediterranean climate is exposed to the South-Asian Monsoon in summer and the Siberian High-Pressure System in winter (Luterbacher, 2005; Lionello et al., 2006). Today, the southern part of the Mediterranean region is mostly influenced by the descending branch of the Hadley cell, while the northern part is more linked to mid-latitude variability, characterized by the North-Atlantic Oscillation (NAO) and other mid-latitude teleconnection patterns (Hurrel et al., 2004).

Thus, ~~climate~~ climate investigations of geological archives of the Mediterranean region reflect paleo-changes in the intensity and extension of global-scale climate patterns. In addition, the Mediterranean sedimentary sequences are characterized by the (quasi-) periodical occurrence of episodes of deep-sea oxygen depletion (sapropel layers) (Olausson, 1991; Rohling et al., 2015 and references therein). Based on their link with the astronomical parameters (Hilgen 1991; Rossignol-Strick, 1983; Lourens 2004; Konijnendijk et al., 2014) these discrete levels represent a useful constraint to establish accurate age ~~models~~ models for marine and land sections.

Formatted: Font: Not Italic

We present a new high-resolution quantitative study of planktonic foraminifera distribution throughout MIS 13-9 for sediment core KC01B collected in the Ionian Sea, central ~~Mediterranean Sea~~Mediterranean Sea. Planktonic foraminifera are amongst the most commonly used proxies for paleoceanographic and paleoclimate sea-surface~~–~~ reconstructions.~~–~~ Their distribution and abundance is strongly linked to surface-water properties. In addition, the physical and chemical properties of their shells reflect ~~the~~ past environmental conditions of the water masses in which they lived (Kucera 2007 and references therein).

The investigated deep-marine sequence of core KC01B represents a key site for stratigraphic and paleoclimatic investigations. This is not only because of its strategic location but also because it was used for the construction of a sapropel-based astronomical timescale for the last 1.1 My (Lourens, 2004). Moreover, in this work, we update the studied time interval ~~studied~~ by using the recent chronological constraints on Pleistocene sapropel deposition (Konijnendijk et al. 2014) ~~and~~ and a new oxygen isotopic record of *N. pachyderma*.

Our main aim is to explore how the ecosystem responded to climate variability during glacial and interglacial intervals throughout MIS 13~~–~~9 in order to discuss the possible mechanisms through which climate acts at the regional and global scale.

In detail, we focus on the main environmental and paleoceanographic processes occurring a) at times of glacial and interglacial MIS; b) during Termination V (T-V) ~~and~~ and Termination IV (T-IV).

2. Modern Oceanographic Setting

Currently, the Mediterranean Sea is an evaporative basin where freshwater loss exceeds freshwater input, forcing an anti-estuarine circulation (Borghini et al., 2014).

~~At~~ At the surface (the first 100-200 m), moderate-salinity Atlantic Water (AW) intrudes through the Strait of Gibraltar and flows to the easternmost part of the Levantine basin ~~while changing~~modifying its temperature and salinity properties (Modified Atlantic Water – MAW). In the intermediate layer (depth between 150–200 and 600 m), Levantine Intermediate Water (LIW) forms in the eastern basin, spreads westwards and continues its flow towards the Strait of Gibraltar, and

then into the Atlantic Ocean (~~Bethoux~~ Béthoux et al., 1992; Robinson et al., 1991; Manca et al., 2004; Malanotte-Rizzoli et al., 2014).

Atmospheric forcing and basin topography determine a large number of local cyclonic and anticyclonic cells (Pinardi and Masetti, 2000). In wintertime, outbreaks of cold and dry continental air masses lead to significant negative heat budgets and buoyancy losses, initiating deep and/or intermediate dense water formation both in the western and in the eastern basins (Malanotte-Rizzoli and Bergamasco, 1991; Castellari et al., 2000).

The Ionian Sea is influenced by the transit and on-site transformation of the major water masses previously described (e.g., Modified Atlantic Water, MAW; Levantine Intermediate water, LIW; and Eastern Mediterranean Deep Water, EMDW, ~~Malonotte~~Malanotte ~~-~~Rizzoli et al., 1997; Napolitano et al., 2000) (Fig. 1). At the near-surface level, most important for biological production, the MAW enters in the western Ionian basin advected by the Atlantic Ionian Stream (AIS) (Fig. 1). Recently, the upper-layer circulation in the Ionian ~~sea~~Sea has been associated with the deep thermohaline circulation through the Bimodal Oscillating System (BiOS): the Ionian upper-layer circulation reverses from cyclonic to anticyclonic and vice versa on decadal time scale affecting the biological productivity in the northern Ionian and southern ~~Adriatic~~ Adriatic Sea (Civitarese et al., 2010; Gačić et al., 2010).

~~The~~ The present-day Mediterranean Sea is characterized by oligotrophic conditions (~~Bethoux~~Béthoux, 1979; Sarmiento et al., 1988~~).~~). The main factor that controls the seasonal change in primary production is linked to the dynamics of the water column with increasing biomass in late winter/early spring and decreasing in summer (Antoine et al., 1995; Bosc et al., 2004; D'Ortenzio and Ribera d'Alcalà, 2009).

A significant West~~-~~-East trophic gradient exists with nutrient depletion (mainly phosphorus) and a reduction in primary productivity in the eastern basin (Krom et al., 1991, 2010).

Moreover, primary productivity reflects the hydrological fragmentation due to mesoscale variability (D'Ortenzio and Ribera d'Alcalà, 2009).

~~An~~ An oligotrophic regime, characterized ~~-~~by a low ~~-~~production, occurs ~~-~~in summer, when ~~-~~a ~~-~~stable stratification takes place (Klein and Coste, 1984; Krom et al., 1992; Crispi et al., 1999; Allen et al.,

2002). During this period, low standing stocks characterize surface waters with the dominance of predatory species. The Ionian planktonic foraminiferal association is generally dominated by *Globigerinoides ruber* pink (40-60%) and *G. ruber* alba (20-40%) with peaks of maximum abundance in the first 50 m of the water column (Pujol and Vergnaud Grazzini, 1995). Winter convection, and less frequently frontal zone migration or upwelling, brings nutrients into the photic zone (mesotrophic regime) (Klein and Coste, 1984). During winter, the assemblage is characterized by the dominance of grazing species such as *Globorotalia truncatulinoides* (50%) and by the presence of other non-spinose species such as *Globorotalia inflata* (20%), and *Globigerina bulloides* (8%). *Globigerinoides ruber* alba (8%) and *Hastigerina siphonifera* (7%) are also part of the association. In detail, *G. inflata* and *G. ruber* alba are more abundant in the first 100 m of the water column, while *G. truncatulinoides* peaks at 200 meters water depth (Pujol and Vergnaud Grazzini, 1995).

The moderate mixing and ventilation processes, occurring during wintertime, bring the nutrients to the photic layer (Napolitano et al., 2000) as documented by the coccolithophorid occurrence in sediment traps collected in this area (Ziveri et al., 2000) and the satellite-derived surface chlorophyll concentration (D'Ortenzio and Ribera d'Alcalà, 2009). This hydrographic/oceanographic feature can also explain the presence of juvenile specimens of *G. inflata* and *G. truncatulinoides* in the surface layer (Pujol and Vergnaud Grazzini 1995).

3. Sediment core

Sediment core KC01B was collected from a small ridge on the lower slope of the southern Calabrian Ridge (Pisano Plateau, 36°15.250' N, 17°44.340' E, 3643 m water depth; Fig. 1) during cruise MD69 of the R/V Marion Dufresne in 1991.

The lithology consists of hemipelagic marls, with intercalation of sapropels and the presence of a number of thin tephra layers and few thin turbidite levels (Castradori 1993; Sanvoisin et al. 1993; Langereis et al. 1997; Lourens 2004).

This 37 m thick sediment sequence represents an invaluable opportunity of investigating the early to late Pleistocene. Core KC-01B has been intensively studied from different points of view, i.e.,

planktonic foraminifera, nannoplankton, stable isotopes, chemical and paleomagnetic analyses, tephra and sapropel presence (Castradori 1993; Sanvoisin et al. 1993; Dekkers et al. 1994, van Santvoort et al. 1997; Langereis et al. 1997; Rossignol-Strick et al. 1998; Rossignol-Strick and Paterne, 1999; Lourens, 2004; Maiorano et al., 2013; Insinga et al. ~~,2014~~, 2014).

Moreover, Core KC01B is well known in the chronostratigraphic literature because it was used for the construction of the Astronomical Time Scale (ATS) (Langereis et al., 1997) in the Mediterranean region and to propose the Tyrrhenian as a regional stage for the Upper Pleistocene (Cita et al., 2005). The ATS is based on the correlation of dominantly precession-controlled sedimentary cycles (*i.e*. sapropels and carbonate cycles) to astronomical parameters~~—~~. In particular, this core was claimed to fill most of the gap between the oldest sapropel (S12) documented in marine sediments (piston core RC9-181 - eastern Mediterranean Sea) dated at 483 ka (Lourens et al., 1996a) and the youngest sapropel (v) exposed in the land-based marine successions of the Vrica section (Southern Italy) dated at 1.280 Ma (Lourens et al., 1996b).

Concomitantly, Rossignol-Strick et al. (1998) proposed an alternative independent age model based on tuning of the oxygen isotope record of KC01B with the ice sheet model of Imbrie and Imbrie (1980).

Differences between both age models are in the order of 0-5 kyr and result from the choice of two different target curves and the adopted time lags between insolation forcing and climate response (Langereis et al., 1997) (for discussion see Hilgen et al., 1993; Lourens et al., 1996a). Largest differences (in the order of 10 kyr) between both age models occur around 618 and 785 ka.

Subsequently, Lourens (2004) established an improved sapropel-tuned age model for this core based on high-resolution colo~~u~~r reflectance correlation with the Ocean Drilling Project (ODP) ~~Site~~ Site 964. This time-scale ~~resulted from~~resulted from a revised chronology of the marine isotope record of Rossignol-Strick et al. (1998), implying a much more uniform change in sedimentation rate for the Ionian Sea cores and a good fit with other Mediterranean and open ocean marine isotope records.

We studied the sediment interval through sections 21-16 of the core (between 21.82 and 15.85 m composite depth, spanning the time interval from 507.3 to 292.1 ka - Lourens, 2004). This interval includes three sapropels (S10, S11 and S12) (Lourens, 2004) (Fig. 2).

4. Methods

Quantitative micropaleontological analyses were performed on 596 samples with a spacing of 1 cm (average time resolution of ~ 380yr). Samples were washed through 63 micron sieves and ~~ovendried~~oven dried at 50°C. Planktonic foraminiferal assemblage composition was determined analysing the >125 μm size fraction. For the micropaleontological census study, each sample was divided with a microsplitter to obtain unbiased aliquots with more than 300 planktonic foraminifers per sample. All taxa are quantified as percentages of the total number of planktonic foraminifers. The faunal data sets described in this paper have been archived, and are available in digital form, at PANGEA.

In this study, *Globigerinoides sacculifer* includes *Globigerinoides trilobus*, *Globigerinoides sacculifer* and *Globigerinoides quadrilobatus* (sensu Hemleben et al., 1989); *Neogloboquadrina pachyderma* sinistral (sin) has been counted separately from the dextral (dex) form.

We distinguished *N. incompta* from *N. pachyderma* by its development of a distinct apertural rim and a more lobulate outline. These taxa showed different vertical distribution and ecology. Studies performed on living planktonic foraminifers in Japan seas and in the eastern North Atlantic document the presence of *N. incompta* in shallower and warmer waters compared to *N. pachyderma* (Kuroyanagi and Kawahata, 2004; Schiebel et al., 2001).

Moreover, different morphotypes of *Globigerinoides ruber* (white) were identified using the morphotype concept of Wang (2000). The typical *Globigerinoides ruber* (d'Orbigny, 1839) is reported as *G. ruber* sensu stricto (s.s.), whereas *Globigerinoides elongatus* (d'Orbigny, 1826) and *Globigerinoides gomitulus* (Seguenza, 1880) are grouped and reported as *G. ruber* sensu lato (s.l.).

Several investigations, based on molecular genetics and geochemistry, highlighted the need to revise the taxonomy of *G. ruber* (d'Orbigny, 1839) which shows remarkable "morphological"

variations (inter alias Darling et al., 1999; Kuroyanagi et al. 2008). In addition, the discrimination of the different morphotypes appears to be necessary because they have significantly different habitat preferences and thus different stable isotopic signals (Wang, 2000; Kuroyanagi and Kawahata, 2004; Loewemark et al., 2005; Kawahata, 2005; Lin and Hsieh, 2007; Numberger et al., 2009). On the other hand, the recent investigation in the Gulf of Mexico of Thirumalai et al. (2014) reports no evidence for discrepancies in s.s.-s.l. calcifying depth habitat or seasonality. The controversial outcomes reported suggest that additional studies ~~on~~ on the relationship between living foraminiferal distribution and oceanographic conditions (productivity, stratification) in different basins are necessary to build a more extensive picture of the ecological requirements of different foraminiferal genetic types~~.~~. In this work, we distinguished between different morphotypes in order to test if they presented different distribution ~~patterns~~ patterns in the past.

The paleoclimate curve was calculated following Cita et al. (1977) and Sanvoisin et al. (1993). It represents the algebraic sum of warm-water species percentages (expressed as positive values) and cold-water species percentages (expressed as negative values) based on ecological preferences and modern habitat characteristics reported in Hemleben et al. (1989), Rohling et al. (1993), and Pujol and Vergnaud-Grazzini (1995). Warm water species are all *G. ruber* (white and pink varieties), *G. sacculifer*, *Globigerinoides tenellus*, *Globigerina rubescens*, *Hastigerina siphonifera* (including *G. calida*) and *Orbulina universa*. The cold water species are *Globigerina bulloides*, *Globigerinita glutinata*, *Globorotalia scitula*, *Turbototalita quinqueloba* and *N. pachyderma* (dex). Negative and positive values of the ~~curve~~ curve allow qualitative estimates for cold and warm surface water respectively.

The paleoproductivity curve is based on a combination of planktonic foraminiferal species: it is calculated as the sum of *G. bulloides*, *G. glutinata* and *T. quinqueloba* percentages. All these taxa are related to high productivity environments (inter alias Bé and Tolderlund, 1971; Fairbanks and Wiebe, 1980; Pujol and Vergaud Grazzini, 1989).

In order to reconstruct paleoenvironmental and paleoceanographical conditions, the relative abundance of some species or groups considered in this study are plotted in percentages with

respect to the total foraminiferal assemblage versus time. We assume that the habitat characteristics of the different species during the Pleistocene were similar to those observed today. Stable isotope analyses were carried out on about 10-15 specimens of the planktonic foraminifers *N. pachyderma* (dex) and *G. ruber* (s.s. and s.l.) (from the >150 μm fraction) using an automated carbonate reaction device Kiel III coupled to a Thermo-Finnigan MAR253 Analytical precision was better than 0.03 and 0.05‰ for $\delta^{13}C$ and $\delta^{18}O$ respectively as deduced from international NBS-19, and in-house Naxos standards.

5. Age control

For the time interval considered in this work (290-510 ka), the age model by Lourens (2004) was partially modified and fine-tuned, considering the new chronological constraints on Pleistocene sapropel depositions (Konijnendijk et al. 2014).

We adopted the revised sapropel chronological framework in the eastern Mediterranean (ODP sites 967 and 968) provided by Konijnendijk et al. (2014) using the highly linear relation between the elemental ratio of titanium and aluminium in the sediment and insolation. The late Pleistocene sapropel chronology of Konijnendijk et al. (2014) presents deviation from Lourens (2004) down to ~400 ka, where sapropel S^b in ODP 967/968 (Emeis et al., 2000) is correlated to one insolation cycle older. Consequently, Sapropel S11 in KC01B [corresponding to sapropel S^b in ODP 967/968 (Konijnendijk et al., 2014)] does not correspond to insolation cycle 38 (as reported in Lourens, 2004 at 407 ka) but to cycle 40 with a corresponding age of 418.9 ka (Konijnendijk et al., 2014).

As additional constraint, we used the tuning of the new high-resolution $\delta^{18}O$ data from *N. pachyderma* (sin) with the open-ocean benthic oxygen isotopic stack from Lisiecki and Raymo (2005) (Fig. 2).

Interpolation between consecutive tie-points was carried out by a linear function, assuming a constant sedimentation rate between the consecutive tie-points (mean sedimentation rate of 0.035 m/ka) and resulted in a higher resolution age control than in previous investigations (Castradori 1993; Sanvoisin et al., 1993; Dekkers et al., 1994, van Santvoort et al., 1997; Langereis et al.,

1997; Rossignol-Strick et al., 1998; Rossignol-Strick and Paterne, 1999). Data used for the age model construction are listed in table 1.

This new Mediterranean $\delta^{18}O$ stack of *N. pachyderma* (dex) in the core KC01B has been compared with the $\delta^{18}O$ data of *G. inflata* of Voelker et al. (2010) from the Atlantic Ocean and with the $\delta^{18}O$ records of *G. bulloides* from ODP-site 975 studied by Pierre et al. (1999) and modified by Lourens (2004) and Kandiano et al. (2012). The good visual comparison between these climatic records supports the adopted age model (Fig. 2).

6. Results

6.1 Foraminiferal assemblages

Foraminiferal assemblages are rich and well preserved. The Shannon-Weaver Index commonly varies between 0.99 and 2.6 (Fig. 3) and exhibits a sharply decreasing trend in diversity during the glacials MIS 12 and MIS 10. The more pronounced minima occur in the upper part of the glacial periods, when more than the 80% of the assemblages is composed by *T. quinqueloba*, neogloboquadrinids (*N. pachyderma* (dex) and *N. dutertrei*) and *G. bulloides* (Fig. 3). The remaining 20% of the assemblages is represented by *G. scitula* and *G. glutinata*. During the interglacials the diversity is higher with dominance of *G. ruber* group (about 50%) and the presence of other warm water taxa such as *O. universa*, *H. siphonifera*, *G.rubescens* and *G. tenellus* (10%). *G. bulloides*, neogloboquadrinids and T. *quinqueloba* show frequencies ranging from 10 to 20%.

The presence of *G. ~~inflata~~ inflata* appears not to be related to glacial-interglacial phases; however higher abundances occur during interglacials (Fig. 3).

A discontinuous pattern is observed in the distribution of *G. sacculifer* and *Globorotalia truncatulinoides*. *G. sacculifer* peaks during interglacial phases with a maximum value of about 20% (Fig. 3). Its distribution is discontinuous during MIS 13, more continuous during MIS 11 and MIS 9. –*G. truncatulinoides* characterises the foraminiferal assemblages during the middle and upper –part of interglacials. The maximum abundance of this taxon (20-25%) is recorded during MIS 11 (Fig. 3).

7. Discussion

7.1 Glacials

Based on the planktonic foraminifera climatic curve, full glacial conditions occur during the upper part of MIS 12 and MIS 10 (Fig. 4). The climate ~~-~~conditions detected during the initial part of MIS 12 and MIS 10 are ~~–~~warmer than expected for a glacial stage as they fall in the range of values prevailing during the previously interglacials MIS 11 and MIS 9 (Fig. 4). These temperatures are principally related to higher percentages of warm surficial waters *G. ruber* group (Fig. 4). At this time, the assemblages are characterized by the dominance of *G. ruber* (s.l.) relative to *G*. *ruber* (s.s.). All these morphotypes occur in tropical-subtropical regions and prefer well-stratified waters but they show different habitats and seasonal preferences. In general, *G. ruber* (s.l.) calcifies deeper than *G. ruber* (s.s.) (Wang, 2000; Lowermark et al., 2005) and reflects different nutrient availability due to stratification of the water column (Lin et al., 2004). Based on the ecological divergence of the morphotypes, we interpret the higher relative abundance of *G. ruber* (s.l.) during the early part of MIS 12 and 10 as indicative primarily of the deepening of the summer thermocline. Probably ~~–~~*G. ruber* (s.l.) has shifted their habitat in order to avoid oligotrophic surface waters documented at this time by the low values of the productivity curve (Fig. 4). In the present Mediterranean Sea, low levels of production occur in summer, when the summer thermocline deepens to ~90 m leading to a stable stratification (Klein and Coste, 1984; Krom et al., 1992). The small differences between $\delta^{18}O$ of *N. pachyderma* and *G. ~~ruber~~ ruber* show that the two taxa share a similar habitat indicating more homogenous conditions during this interval between surface and intermediate waters (Fig. 4).

The climatic conditions detected during early MIS 12 in core KC01B are coeval with the relative wintertime warmer sea surface temperatures (SST) documented in the nearshore waters off Portugal and in the western Mediterranean basin by Voelker et al. (2010) and associated with the increased heat transport by the Azores Current across the Atlantic. Moreover, the warming detected during the lower half of MIS 10 displays the same warm temperature anomaly in the SST record ~~-~~of Site 980 (North Atlantic, Feni Drift) (McManus et al., 1999) and site 1089 (South Atlantic Subtropical Front) (Cortese et al., 2007) during full glacial MIS 10 centered at ca. 350 ka and ~~-~~linked

by the authors to a stronger than usual Agulhas Current influence. These similarities can be explained by the quick response of sub-surficial Mediterranean waters to atmospheric processes during both glacial stages. The warming occurring during the glacial half of both glacial MIS 10 and MIS 12 implies an extra-regional connection between the Mediterranean sea and the northern and southern hemisphere.

The subsequent increase in abundances of cold water indicators *T. quinqueloba*, *N. pachyderma* (dex) and *G. bulloides* document the establishment of full glacial conditions during MIS 12 and MIS 10 at about 455 ka and 360 ka, respectively (Fig. 4). Well known environmental preferences of these species for nutrient-rich environments (Be and Tolderlund, 1971; Fairbanks and Wiebe, 1980; Reynolds and Thunell, 1986; Pujol and Vergnaud-Grazzini, 1995; Sierro et al., 2003) suggest productive sea surface waters as also supported by the highest values of the paleoproductivity curve (Fig. 4). At this time the fertilization can be triggered by the concurrence of different factors. One is represented by eolian input due to enhanced North-African dust deposition in the eastern Mediterranean (Roberts et al., 2011) during the upper part of the last five glacial stages. However, the eolian dust in general does not seem able to provide an adequate and/or continuous source of nutrients to enhance primary production (Krom et al., 2005; Incarbona et al., 2008). Another important factor may be the higher buoyancy gradient due to the reduced Atlantic surface-waters inflow that has altered the equilibrium of vertical mixing in the water column.

The glacial sea-level lowstand at the time of MIS 12 and MIS 10, leads to a reduced Atlantic surface-water influx and thus to shoaling of the density gradient (pycnocline) between intermediate and surface waters within the Mediterranean. This shoaling is similarly to what has been suggested for other glacial sea-level lowstands (Rohling and Gieskes, 1989; Rohling, 1991; Rohling and Bryden, 1994; Myers et al., 1998).

This factor is more evident during MIS12 when sea level was about 125 m below present (Rohling et al., 2009) (Fig. 4). MIS 12 is generally dominated by higher abundances (respect compared to MIS 10) of *N. pachyderma* (dex) and *N. dutertrei* reaching up to 60 % of the total assemblage. These taxa are indicative of for the intensity of the deep chlorophyll maximum (DCM), and occursoccurring when the upper part of the water column is isothermal and cold (Rohling and

Gieskes, 1989; Pujol and Vergnaud Grazzini, 1995). Such DCM may develop during periods of reduced deep mixing. ~~A similar~~Similar evidence comes from the offset observed between *N. pachyderma* and *G. ruber* oxygen isotope values (Fig. 4) that document ~~a stratification~~stratification between the surficial and the lower part of the photic zone. This is ~~consistenty~~consistent~~ly~~ with a different density gradient in the water column due to ~~-~~the large decrease in Atlantic surface ~~inflow~~ ~~.~~inflow.

The colder intervals of the investigated glacials are characterized by peaks in abundance~~s~~ of *N. pachyderma* (sin) (with values of 18%) at times of extremely negative, cold values of the climate curve (Fig. 5). *N. pachyderma* (sin) is known not only to prefer polar-subpolar waters (Hemleben et al., 1989; Bé and Tolderlund, 1971; Reynolds and Thunell, 1986; Dieckmann et al., 1991; Johannessen et al., 1994), but also to be the dominant planktonic foraminiferal species during Heinrich events recorded in the North Atlantic ~~ocean~~Ocean (Heinrich, 1988; Bond et al., 1992).

Very rare specimens of *N. pachyderma* (sin) have been towed at the end of summer in the Ionian Sea (Pujol and Vergnaud-Grazzini, 1995); however this taxon is generally uncommon ~~-~~(<5%) in the Mediterranean during the Quaternary (Thunell, 1978; Rohling and Gieskes, 1989; Rohling et al., 1993; Hayes et al., 1999; Sprovieri et al., 2003; Hayes et al., 2005; Triantaphyllou et al., 2009; Siani et al., 2010~~,~~ ; Sprovieri et al., 2012). ~~-~~Significant percentages of *N. pachyderma* (sin) in the western Mediterranean Sea during the last glacial period have been interpreted as the result of polar water intrusions into the Mediterranean via the Strait of Gibraltar at ~~-~~the time of the Atlantic Heinrich events (Cacho et al., 1999; Pérez-Folgado et al., 2003; Sierro et al., 2005). The increases in the relative abundance of *N. pachyderma* (sin), coeval with a SST drop comparable for distribution and amplitude to the Heinrich-type events, have also been documented during MIS5 (Combourieu Neobout et al., 2002; Martrat et al., 2004), throughout MIS 15-9 (Girone et al., 2013) and during MIS 100 (Becker et al., 2006) in the western and eastern basin.

At the investigated site (Fig. 5), we observe that the distribution of *N. pachyderma* (sin) is positively correlated with that of neogloboquadrinids and that, despite the different time-resolution of the data, the significant increase in abundance of *N. pachyderma* (sin) correlates well with that observed in the western Mediterranean (ODP Site 975) (Girone et al., 2013) and North Atlantic

Heinrich-type events (Stein et al., 2009; Rodrigues et al., 2011). In the Mediterranean Sea high abundances of neogloboquadrinids are often associated with low-density water masses as observed in sapropel deposition during colder climatic phases (Capotondi and Vigliotti, 1999; Negri et al., 1999; Stefanelli et al., 2005). We can speculate that the cooling of Atlantic inflowing waters due to iceberg melting, already documented in the western Mediterranean (Sierro et al., 2005; Frigola et al., 2008), could also have affected the hydrological setting of the Ionian Sea. On the other hand, this may have occurred because of the intense freshwater discharges into the Mediterranean through the Black Sea from meltwater of lakes dammed by the Scandinavian ice sheet (Sprovieri et al., 2012) and/or from NW African (Atlas) mountain glaciers (Rogerson et al., 2008). At ~~the~~ present, we do not have clear evidence~~s for of a~~ local source~~s~~ of water~~; and~~ further high-resolution studies are necessary to understand the occurrence and distribution of *N. pachyderma* (sin) in the Mediterranean Sea.

7.2 Interglacials

From the paleoclimatic curve ~~During MIS 11~~ typical full interglacial conditions can for the first time be recognized during MIS 11 at ~~around~~ ~420 ka ~~on the paleoclimatic curve~~.

The warm conditions culminate between 415 to 395 ka when the microfauna is characterized by the presence of ~~the~~ tropical ~~-~~ subtropical species *G. sacculifer* that prefers warmer and shallower waters than *G. ruber* (Kuroyanagi and Kawahata, 2004). At present, this species lives in the western Mediterranean at the end of summer (Pujol and Vergnaud-Grazzini, 1995) and its distribution in surface sediments from west to east reflects its strong temperature dependence (Thunel, 1978). The increase in abundance of *G. sacculifer* in the Mediterranean has been reported to be associated to “Climatic Optima” during the late Holocene intervals e.g. Medieval Warm Period, the Roman Age, the late Bronze Age and the Copper Age (Piva et al., 2008; Lirer et al., 2013; 2014). According, we interpret the occurrence of this species in core KC01B during interglacial MIS 11 and MIS 9 as indicative of the “Climatic Optimum interval/Thermal maximum”. This interpretation concurs with the paleoclimate reconstruction of the same period and for the same core, based on calcareous nannofossil assemblages (Maiorano et al., 2013). ~~.~~ The presence

of an extended “Climatic Optimum”, lasting ~30 ka, has been documented in SST records across the world ocean (McManus et al., 1999; Hodell et al., 2000; De Abreu et al., 2005; Kandiano and Bauch, 2007; Dickson et al., 2009; Stein et al., 2009; Voelker et al., 2010), from Antarctic ice cores (Petit et al., 1999; Jouzel et al., 2007) and in terrestrial pollen records (Tzedakis, 2010~~).~~). It occurs after a prolonged deglacial warming ~~–~~(Termination ~~I~~V) that extends into MIS 11 with global and regional climate variability (Milker et al., 2013 and references therein).

The present ~~–~~high-resolution database provides new climatostratigraphic insights for the “Climatic Optimum” of the central Mediterranean region. It is interesting to note that, during MIS 11, *G. sacculifer* shows three different ~~-~~peaks of abundance concomitant with the decrease/absence of *G. truncatulinoides* ~~–~~(Fig. 4). *G. sacculifer* reaches its maximum quantity in the Eastern Basin, where surface waters remain relatively warm, and low nutrient contents prevail throughout the year due to the a relatively stable ~~-~~pycnocline at depth (Pujol and Vergnaud Grazzini, 1995).

Higher values of living *G. truncatulinoides* have been observed in the Mediterranean in ~~–~~areas of intense water mixing during winter, i.e. the North Western Basin (Pujol and Vergnaud Grazzini, 1995), while in the more stratified waters of the Eastern Basin it is rarely found (Core top database of Kallel et al. (1997).

Distributional trends of these taxa document that the “Climatic Optimum” of MIS 11 was not uniform but characterized by three distinct intervals with a year-around water column stratification and/or a weaker winter mixing with a consequent limited food supply. At the same time, higher values of the paleoclimate curve imply warmer superficial conditions ~~–~~or elevated winter sea surface temperatures (i.e. increase of the warm water taxa). The three warmer intervals present an estimated age of 415-410 ka, 408-403 ka, ~~400~~and 400-395 ka, respectively.

An interesting remark is that the peak from 400 to 395 ka is coeval with and shows the same length of the warm interval (400-395 ka Fig. 4) recorded in marine paleoclimate data off Iberia at the end of the MIS 11c (Koutsodendris and Zahn, 2014). ~~–~~Since that interval corresponds to an insolation minimum, this implies that orbital insolation forcing is not the warming cause.

Koutsodendris and Zahn ~~–~~(2014) motivate the North-Atlantic warmth as an interhemispheric teleconnection between strong leakage in the South Atlantic and Atlantic Meridional Overturning

Circulation (AMOC)-driven warmth in the North Atlantic maintaining temperate conditions off Iberia and the continental Europe during the MIS11c. Accordingly, we speculate that the warmer intervals identified in our record are the result of an ocean-climate teleconnection between the high- and low- latitudes. Nevertheless, additional sites are necessary in order to understand the exact mechanisms and extent of such climatic variability at time of the "Climatic Optimum".

The observed post-glacial temperature increase after Termination V does not match the Holocene SST trend when the "Climatic Optimum" already began after Termination I coincident with Sapropel S_1 deposition (Rohling and De Rijk, 1999; Capotondi et al., 1999; Cacho et al., 2001; Triantaphyllou et al., 2009). However a direct comparison between MIS 11 and MIS 1 is difficult to make because of a different phase in the orbital parameters. In fact, the present interglacial (Holocene) spans a single summer insolation maximum (summer at 65° N), while MIS 11 interglacial optimum spans two (weak) insolation maxima (Laskar et al., 2004).

From 392 ka onward, the MIS11 in core KC01B is characterized by oligotrophic surface waters during summer (Fig. 4) and eutrophic during winter, when deep-water masses are well-ventilated, as testified by the presence of *G. inflata* and *G. truncatulinoides*. These conditions are comparable to those in the present-day Ionian Sea. At present, *G. inflata* and *G. truncatulinoides* dominate the fauna of the winter assemblages in the Ionian Sea (Pujol and Verganud Grazzini, 1995). Distribution of planktonic foraminifera during MIS 9 document similar general trends as described for MIS 11, with a thermal maximum between 326 and 320 ka (Fig.4). However, MIS9 is characterized by lower percentages of warm-water taxa compared to MIS 11, thus suggesting that SSTs were lower during MIS9 than during MIS11.

7.3 Sea surface changes during transition T-V and T-IV

Termination V in core KC01B is marked by a decrease of $\delta^{18}O$ of *N. pachyderma* from +2.5‰ at 430 ka to +0.8 ‰ at 420 ka (Fig. 6). During this transition the planktonic foraminifera content shows significant changes related to different environmental conditions (Fig. 6) and provides new data on how the transitions evolved from glacial to interglacial.

The high abundance of the herbivorous species *G. bulloides* and *T. quinqueloba* from ~430 to ~425 ka (Fig. 6) suggests enhanced nutrient supply in the sub-surface water masses. As these species reach the highest concentrations in upwelling regions or in areas of vigorous vertical mixing in the water column (Reynolds and Thunell, 1986), where high phytoplankton productivity prevails, we can hypothesize the presence of an upwelling regime or continental coastal input at this time, probably induced by the presence or intensification of the gyre similar to the one observed at present in the Ionian Sea (Civitarese et al., 2010, Gacic et al., 2010). The absence of *G. ~~inflata~~inflata* (Fig. 4) supports this oceanographic scenario, as this species prefers temperate and high nutrient waters not affected by upwelling processes (Giraudeau 1993. The increase in primary productivity is also documented by the calcareous nannofossil data (Maiorano et al., 2013). This phase is coeval with a peak of iron-rich terrigenous dust at ODP Site 958 (Helmke et al., 2008), related to the strengthening of trade winds over northwestern Africa. Probably, this strengthening of westerlies is also associated with the strengthening of the Atlantic Ionian Stream jet leading to a dynamic activity of mesoscale features such as meanders and eddies. The latter results in mixing thus in enhanced nutrient supply, and leads to increased ~~enhanced~~ primary production. Several oceanographic studies performed in different areas of the Mediterranean document~~ed~~ that ~~the~~ variability in mesoscale hydrographic features leads to an increase of biological productivity (Estrada, 1996; Christaki et al., 2011).

The relatively low abundance of *G. bulloides* between 424 and 420 ka, together with the increasing percentages of *N. pachyderma* (dex) and *N. dutertrei* (Fig. 6)~~.~~ documents the transition to stratified water conditions and the development of a DCM. The co-occurrence of *N. incompta, a species* that prefers shallower and warmer waters than *N. pachyderma* (Kuroyanagi and Kawahata, 2004), also suggests amelioration of climate (Fig. 6).

We interpret this microfaunal assemblage as the result of fresh-water input/land-derived nutrients associated with the climatic transition from glacial conditions of MIS 12 to the interglacial conditions of MIS 11. Further evidence is provided by the steadily decreasing $\delta^{18}O$ of *N. pachyderma* during the same period (Fig. 6), which might be explained by a SST increase or a salinity decrease due to surface water freshening during this phase.

The increase in *G. ruber* abundance at around 420 ka together with ~~ligher~~lighter oxygen isotopic values in *N. pachyderma* reflects the influence of the African humid phase in the Ionian sea that culminates with sapropel layer S11 deposition at 418.9 ka (Konijnendijk et al., 2014) (Fig. 6). This is suggested by the ~~coherent~~ timing that is coherent with the onset of the wet phase over North-West Africa (Helmeke et al., 2008), when the enhanced influence of the West African Monsoon system on the Saharan-Sahel region led to higher fresh-water input into the Mediterranean. During the early MIS 11 the African monsoon system intensification is also documented in marine records from the North Atlantic and western Mediterranean ~~sea~~Sea and it has been related to the northward-moving of the Intertropical Convergence Zone (ITCZ) (Kandiano et al., 2012).

In general, changes in the planktonic foraminiferal distribution observed during transition T-IV lead to a similar climatic reconstruction as outlined for T-V (Fig. 6). The dominance of *G. bulloides* and *T. quinqueloba* from 342 to ~~–~~ 337 ka points to enhanced nutrient content and mixing/upwelling during the first part of the transition from MIS 10 to MIS9. The subsequent replacement (~ 336-333 ka) of *N. pachyderma* and *N. dutertrei* suggests stratified conditions with a shallow mixed layer ~~low surficial water masses~~. Then, Sapropel S10 occurs at 332 ka (Konijnendijk et al. 2014) (Fig. 6).

Based on our data, the dynamics of the sea surface property during Termination V are due to the deglaciation and wind system variability. The timing and modalities of climate dynamics during the Terminations in different regions are as yet not fully understood. Recent investigations focus on the relative position of the Heinrich cold events that characterize all last five Terminations at a global scale (Cortese et al., 2007; Cheng et al., 2009; Barker et al., 2011; Marino et al., 2015). During the most recent Terminations I (MIS 2/MIS 1) and II (MIS 6/MIS 5) their positions show strong differences in these two deglaciations and ~~evidence that~~point to a bipolar seesaw control~~s~~ ~~the~~ mechanism ~~of~~ for ~~termination~~ Termination II (Marino et al., 2015).

Observing the distributional trend of *N. pachyderma* (sin) in core KC01B, a “Heinrich-like” cold event (see paragraph above) is clearly detected within both the ~~Transitions~~ transitions T-V and T-IV (Fig. 6) in correspondence with a small drop in the oxygen isotope record (Fig. 6). Based on paleoceanographic inferences provided by planktonic foraminifera, these cold episodes occur

Formatted: Not Highlight

Formatted: Not Highlight

approximately in the mid-point of the deglaciations, coincident with the increase in trade wind intensity off NW Africa (Fig. 6). This suggests that they are probably linked to the wind influence and ~~so~~ thus to ~~the~~ atmospheric conditions.

This interpretation is also consistent with reported results from other ocean basins, indicating that Heinrich-like events are associated with stronger winds (e.g. Wang et al., 2001; Moreno et al., 2002; Itambi et al., 2009; Roberts et al., 2011). These are ~~and~~ probably induced by southward shifts of the Inter Tropical Convergence Zone (Jullien at al., 2007).

Accordingly, we conclude that the T-V and T-IV observed in the Mediterranean are not only regional events but are associated with a dynamic reorganization of global atmospheric conditions. Our environmental scenarios are consistent with the sequence of major events documented in the last four Terminations that link the displacements of the ITCZ, the AMOC and the North Atlantic cooling (Cheng et al., 2009; Schneider et al., 2014; Marino et al., 2015).

During glacial-interglacial transitions T-IV and T-V the climate/ocean interaction was probably related to strong feedback processes: the weakening or shutdown of the ~~Atlantic Meridional Overturning Circulation (~~AMOC~~)~~ due to ~~the~~ enhanced freshwater input to the North Atlantic resulted in an increase in sea surface temperature within the tropics as well as in cooling of the North Atlantic and in the geographical shift of the wind system over North Africa.

Clearly, more data with good age control are needed from a wider area so to substantiate and evaluate extent and intensity of these events. This is not only needed to better understand mechanisms of paleo-climate change but is also relevant for our abilities to forecast potential future climate change processes.

8. Conclusions

A detailed study on planktonic foraminiferal assemblages from sediment core (KC01B) collected in the Ionian Basin (central Mediterranean Sea) allowed us to reconstruct the climate variability during glacial- interglacial periods between 500 and 300 ka (MIS 13 - MIS9). The main results can be summarized as follows:

- The early part of MIS 12 and MIS 10 is characterized by relatively “warm conditions” with a deepening of the summer thermocline -derived from the quantitative distribution of *G. ruber* s.l. with respect to *G. ruber* s.s. Glacial conditions and eutrophic regimes are established in the upper half of the interval evidenced by significant increase of *T. quinqueloba*, N*. pachyderma* (dex) and *G. bulloides*. The colder intervals are interrupted by peaks in abundance of *N*. *pachyderma* (sin) coeval with north-Atlantic Heinrich-type cold events suggesting the close association of Central Mediterranean climate and North-Atlantic millennial-scale climate instability.

- Interglacials MIS 11 and MIS 9 have a prolonged “Climatic Optimum” lasting ~20 and 6 Ka respectively, as documented -by the increase of the warm species *G. sacculifer*. -Here for the first time we document that the extended warmth during the MIS 11c is characterized by three intervals with elevated -winter sea surface temperatures -and a weaker winter mixing.

- Complex paleoceanographic changes occurred during the glacial - interglacial transitions (T-V and T-IV) consistent with the sequence of major events documented in the last four Terminations that link the displacements of the ITCZ, the AMOC and the North Atlantic cooling.

The high-resolution investigations allow -us to provide the timing of these changes occurring in the Mediterranean region and to link these to global climate events.

Acknowledgements

The authors acknowledge L. van Roij, A. Filippidi, and A. van Dijk for isotope measurements. Special thanks go to two anonymous reviewers and the editor Paul Hesse for their helpful comments and suggestions. ~~and the editor (Paul Hesse).~~ Discussions with E. Bonatti, L. Vigliotti and P. Montagna are gratefully acknowledged. This study was financially supported by NWO (PASSAP, PASS), EU-Mast (Paleoflux), NEXTDATA and RITMARE (Ricerca ITaliana per il MARE) projects. This is contribution number 1873 of the CNR-ISMAR of Bologna.

References

Allen, J.I., Somerfield, P.J., Siddorn, J., 2002. Primary and bacterial production in the Mediterranean Sea: a modelling study. Journal of Marine Systems 33-34, 473-495.

584 Antoine, D., Morel, A., André, J.M., 1995. Algal pigment distribution and primary production in the
585 Eastern Mediterranean as derived from Coastal Zone Color Scanner observations. Journal of
586 Geophysical Research, 100, 16193-16209.

587 Barker, S., Knorr, G., Edwards, R.L., Parrenin, F., Putnam, A.E., Skinner, L.C., Wolff, E., Ziegler,
588 M., 2011. 800,000 Years of Abrupt Climate Variability. Science 347, 0-5.

589 Bauch, H.A., Erlenkeuser, H., Helmke, J.P., Struck, U., 2000. A paleoclimatic evaluation of marine
590 oxygen isotope stage 11 in the high-northern Atlantic (Nordic seas). Global and Planetary Change
591 24, 27-39.

592 Bè, A.W.H., Tolderlund, D.S., 1971. Distribution and ecology of living planktonic foraminifera in
593 surface waters of the Atlantic and Indian Oceans. In: Funnel, B.M., Riedel, W.R. (Eds.). The
594 Micropaleontology of Oceans. Cambridge University Press, Cambridge, pp. 105-149.

595 Becker, J.F., Lourens, L.J., Raymo, M.E., 2006. High-frequency climate linkages between the
596 North Atlantic and the Mediterranean during marine oxygen isotope stage 100 (MIS100).
597 Paleoceanography 21, PA3002, http://dx.doi.org/ 10.1029/2005PA001168.

598 ~~Bethoux~~Béthoux, J.P., 1979. Budgets of the Mediterranean Sea. Their dependence on the local
599 climate and on the characteristics of the Atlantic waters. Oceanologica Acta 2, 157-163.

600 B~~é~~éthoux, J.P., Morin, P., Madec, C., Gentili, B., 1992. Phosphorus and nitrogen behaviour in the
601 Mediterranean Sea. Deep-Sea Research 39, 1641-1654.

602 B~~e~~éthoux, J.P., Gentili, B., Morin, P., Nicolas, E., Pierre, C., Ruiz-Pino, D., 1999. The
603 Mediterranean Sea: a miniature ocean for climatic and environmental studies and a key for the
604 climatic functioning of the North Atlantic. Progress in Oceanography 44, 131-146.

605 Bond, G., Heinrich, H., Broecker, W., Labeyrie, L., McManus, J., Andrews, J., Huon, S., Jantschik,
606 R., Clasen, S., Simet, C., Tedesco, K., Klas, M., Bonani, G., Ivy, S., 1992. Evidence for massive
607 discharges of icebergs into the North Atlantic Ocean during the last glacial period. Nature 360,
608 245-249.

609 Borghini, M., Bryden, H., Schroeder, K., Sparnocchia, S., Vetrano, A., 2014. The Mediterranean is
610 becoming saltier. Ocean Science 10, 693–700.

611 Bosc, E., Bricaud, A., Antoine, D., 2004. Seasonal and interannual variability in algal biomass and
612 primary production in the Mediterranean Sea, as derived from 4 years of SeaWiFS observations,
613 Global Biogeochemical Cycles 18, GB1005.

614 Cacho, I., Grimalt, J., Pelejero, C., Canals, M., Sierro, F.J., Flores, J.A., Shackleton, N., 1999.
615 Dansgaard-Oeschger and Heinrich event imprints in Alboran Sea paleotemperatures,
616 Paleoceanography 14(6), 698–705.

617 Cacho, I., Grimalt, J.O., Canals, M., Sbaffi, L., Shackleton, N.J., Schònfeld, J., Zahn, R., 2001.
618 Variability of the western Mediterranean Sea surface temperatures during the last 25,000 years
619 and its connection with the northern hemisphere climatic changes. Paleoceanography 16, 40-52.

620 Capotondi, L., Borsetti, A.M., Morigi, C., 1999. Foraminiferal ecozones, a high resolution proxy for
621 the late Quaternary biochronology in the central Mediterranean Sea. Marine Geology 153, 253-
622 274.

623 Capotondi, L., Vigliotti, L., 1999. Magnetic and microfaunistical characterization of late Quaternary
624 sediments in the Western Mediterranean (ODP Leg 161). Inference on sapropel formation and
625 paleoceanographic evolution. In: Zahn, R., Comas, M.C., and Klaus, A. (Eds.) Proceedings of the
626 Ocean Drilling Program, Scientific Results, College Station TX, 161, 505-518.

627 Castellari, S., Pinardi, N., Leaman, K., 2000. Simulation of water mass formation processes in the
628 Mediterranean Sea: influence of the time frequency of the atmospheric forcing. Journal of
629 Geophysical Research 105, 24157-24181.

630 Castradori, D., 1993. Calcareous nannofossils and the origin of eastern Mediterranean sapropels.
631 Paleoceanography 8, 459-471.

632 Cheng, H., Edwards, R.L., Broecker, W.S., Denton, G.H., Kong, X., Wang, Y., Zhang, R., Wang X.,
633 2009. Ice age terminations. Science 326, 248–252.

634 Christaki, U., Van Wambeke, F., Lefevre, D., Lagaria, A., Prieur, L., Pujo-Pay, M., Grattepanche,
635 J.-D., Colombet, J., Psarra, S., Dolan, J.R., Sime-Ngando, T., Conan, P., Weinbauer, M.G.,
636 Moutin, T., 2011. The impact of anticyclonic mesoscale structures on microbial food webs in the
637 Mediterranean Sea. Biogeosciences Discuss 8, 185-220.

638 Cita, M.B., Vergnaud-Grazzini, C., Robert, C., Chamley, H., Ciaranfi, N., D' Onofrio, S., 1977.
639 Paleoclimatic record of a long deep-sea core from the eastern Mediterranean. Quaternary
640 Research 8, 205-235.

641 Cita Sironi, M.B., Capotondi, L., Asioli, A., 2005. The Tyrrhenian stage in the Mediterranean:
642 definition, usage and recognition in the deep-sea record. Rendiconti Accademia Lincei 9, 16, 297-
643 310.

644 Civitarese, G., Gačić, M., Lipizer, M., Eusebi Borzelli, G.L., 2010. On the impact of the Bimodal
645 Oscillating System (BiOS) on the biogeochemistry and biology of the Adriatic and Ionian Seas
646 (Eastern Mediterranean). Biogeosciences 7, 3987–3997.

647 Combourieu Nebout, N., Turon, J.L., Zahn, R., Capotondi, L., Londeix, L., Pahnke, K., 2002.
648 Enhanced aridity and atmospheric high-pressure stability over the western Mediterranean during
649 the North Atlantic cold events of the past 50 ky. Geology 30, 863–866.

650 Cortese, G., Abelmann, A., Gersonde, R., 2007. The last five glacial-interglacial transitions: A high-
651 resolution 450,000-year record from the subantarctic Atlantic. Paleoceanography 22 (4), PA4203.

652 Crispi, G., Crise, A., Mauri, E., 1999. A seasonal three-dimensional study of the nitrogen cycle in
653 the Mediterranean Sea: part II. Verification of the energy constrained trophic model. Journal of
654 Marine Systems 20, 357-380.

655 Darling, K.F., Wade, C.M., Kroon, D., Leigh Brown, A.J., Bijma, J., 1999. The diversity and
656 distribution of modern planktic foraminiferal small subunit ribosomal RNA genotypes and their
657 potential as tracers of present and past ocean circulations. Paleoceanography 14, 3-12.

658 De Abreu, L., Abrantes, F., Shackleton, N., Tzedakis, P.C., McManus, J.F., Oppo, D.W., Hall, M.A.,
659 2005. Ocean climate variability in the eastern North Atlantic during interglacial marine isotope
660 stage 11: a partial analogue for the Holocene? Paleoceanography 20, PA3009.
661 doi:10.1029/2004PA001091.

Dekkers, M.J., Langereis, C.G., Vriend, S.P., Van Santvoort, P.J.M., De Lange, G.J., 1994. Fuzzy c-means cluster analysis of early diagenetic effects on natural remanent magnetisation acquisition in a 1.1 Myr piston core from the central Mediterranean. Physics of the Earth and Planetary Interiors 85, 155-171.

Dickson, A.J., Beer, C.J., Dempsey, C., Maslin, M.A., Bendle, J.A., McClymont, E.L., Pancost, R.D., 2009. Oceanic forcing of the Marine Isotope Stage 11 interglacial. Nature Geoscience 2, 428-433.

Dieckmann, G.S., Spindler, S., Lange, M.A., Ackley, S.F., Eicken, H., 1991. Antarctic sea ice: A habitat for the foraminifer Neogloboquadrina pachyderma, Journal of Foraminiferal Research 21,181-194.

d'Orbigny, A.D., 1826. Tableau méthodique de la classe de céphalopodes. Annales Des Sciences Naturelles 14, 1–277.

d'Orbigny A.D., 1839. Mollusques, echinodermes, foraminiferes et polypiers, recueillis aux illes Canaries par Mm. Webb et Berthelot et décrits par Alcide D'Orbigny (2éme partie: Mollusques). Paris: 117 pp.; 8 pls.

D'Ortenzio, F., Ribera d'Alcalà, M., 2009. On the trophic regimes of the Mediterranean Sea: a satellite analysis. Biogeosciences 6, 139–148.

Emeis, K.C., Struck, U., Schulz, H.M., Rosenberg, M., Bernasconi, S.M., Erlenkeuser, H., Sakamoto, T., Martinez-Ruiz, F.C., 2000. Temperature and salinity variations of Mediterranean Sea surface water over the last 16,000 years from records of planktonic stable oxygen isotopes and alkenone unsaturation ratios. Palaeogeography, Palaeoclimatology, Palaeoecology-158 (3-4), 259-280.

EPICA community members, 2004. Eight glacial cycles from an Antarctic ice core. Nature 429, 6992, pp.623-628.

Estrada, M., 1996. Primary production in the northwestern Mediterranean. Science Marine 60 (Suppl. 2), 55-64.

Fairbanks, R.G., Wiebe, P.H., 1980. Foraminifera and chlorophyll maximum: vertical distribution, seasonal succession, and paleoceanographic significance. Science 209, 1524–1526.

Frigola, J., Moreno, A., Cacho, I., Canals, M., Sierro, F.J., Flores, J.A., Grimalt, J.O., 2008. Evidence of abrupt changes in Western Mediterranean Deep Water circulation during the last 50 kyr: a high-resolution marine record from the Balearic Sea. Quaternary International 181, 88–104.

Gačić, M., Borzelli, G. L. E., Civitarese, G., Cardin, V., Yari, S., 2010. Can internal processes sustain reversals of the ocean upper circulation? The Ionian Sea example. Geophysical Research Letters *37* (9), 1-5.

Giraudeau, J., 1993. Planktonic foraminiferal assemblages in surface sediments from the southwest African margin. Marine Geology 110, 47-62.

Girone, A., Capotondi, L., Ciaranfi, N., Di Leo, P., Lirer, F., Maiorano, P., Marino, M., Pelosi, N., Pulice, I., 2013. Paleoenvironmental changes at the lower Pleistocene Montalbano Jonico section (southern Italy): Global versus regional signals. Palaeogeography, Palaeoclimatology, Palaeoecology 371, 62–79.

Hayes A., Rohling E.J., De Rijk S., Kroon D., Zachariasse W.J., 1999. Mediterranean planktonic foraminiferal faunas during the last glacial cycle. Marine Geology 153, 239–252.

Hayes, A., Kucera, M., Kallel, N., Sbaffi, L., Rohling, E.J., 2005. Glacial Mediterranean sea surface temperature based on planktonic foraminiferal assemblages. Quaternary Science Review 24, 999-1016.

Heinrich, H., 1988. Origin and consequences of cyclic ice rafting in the northeast Atlantic Ocean during the past 130,000 years. Quaternary Research 29, 142–152.

Helmke J.P. and Bauch, H.A., 2003. Comparison of conditions between the polar and subpolar North Atlantic region over the last five climate cycles. Paleoceanography 18, 2, 1036.

Helmke, J.P., Bauch, H. A., Röhl, U., Kandiano, E.S., 2008. Uniform climate development between the subtropical and subpolar northeast Atlantic across marine isotope stage 11–. Climate of the Past 4, 181-190.

Hemleben, C., Spindler, M., Anderson, O.R., 1989. Modern Planktonic Foraminifera. Springer, New York, pp. 1-363.

Hilgen, F.J., 1991. Astronomical calibration of Gauss to Matuyama sapropels in the Mediterranean and implication for the Geomagnetic Polarity Time Scale. Earth Planetary Science Letters 104, 226–244.

Hilgen, F.J., Lourens, L.J., Berger, A., Loutre, M.F., 1993. Evaluation of the astronomically calibrated time scale for the late Pliocene and earliest Pleistocene. Paleoceanography 8, 549–565.

Hodell, D.A., Charles, C.D., Ninneman, U.S., 2000. Comparison of interglacial stages in the South Atlantic sector of the southern ocean for the past 450 ka: implications for marine isotope stage (MIS) 11. Global and Planetary Change 24 (1), 7-26.

Hurrell, J.W., Hoerling, M.P., Phillips, A.S., Xu, T., 2004. Twentieth century North Atlantic climate change. Part I: assessing determinism. Climate Dynamics 23, 371-389.

Imbrie, J., Imbrie, J. Z., 1980. Modeling the climatic response to orbital variations, Science, 207, 943– 953.

Incarbona, A., Di Stefano, E., Sprovieri, R., Bonomo, S., Censi, P., Dinarès-Turell, J., Spoto, S., 2008. Variability in the vertical structure of the water column and paleoproductivity reconstruction in the central-western Mediterranean during the Late Pleistocene. Marine Micropaleontology 69 (1), 26-41.

Insinga, D.D., Tamburrino, S., Lirer, F., Vezzoli, L., Barra, M., De Lange, G.J., Tiepolo M., Vallefuoco M., Mazzola, S., Sprovieri, M., 2014. Tephrochronology of the astronomically-tuned KC01B deep-sea core, Ionian Sea: insights into the explosive activity of the Central Mediterranean area during the last 200 ka. Quaternary Science Reviews 85, 63–84.

Itambi, A.C., von Dobeneck, T., Mulitza, S., Bickert, T. and Heslop, D., 2009. Millennial-scale northwest African droughts related to Heinrich events and Dansgaard-Oeschger cycles: Evidence in marine sediments from offshore Senegal. Paleoceanography 24: doi: 10.1029/2007PA001570.

Jansen, J.H.F., Kuijpers, A., Troelstra, S.R., 1986. A Mid- Brunhes climatic event: Long term changes in global atmo- spheric and ocean circulation. Science 232, 619-622.

Johannessen, T., Jansen, E., Flatøy, A., Ravelo, A. C., 1994. The relationship between surface water masses, oceanographic fronts and paleoclimatic proxies in surface sediments of the Greenland, Iceland, Norwegian seas. In Carbon Cycling in the Glacial Ocean: Constraints on the Ocean's Role in Global Change, NATO ASI Ser. I 117, Zahn, R. et al. (Eds), Springer, Berlin, pp. 61-86.

Jouzel, J., Masson-Delmotte, V., Cattani, O., Dreyfus, G., Falourd, S., Hoffmann, G., Minster, B., Nouet, J., Barnola, J.M., Chappellaz, J., Fischer, H., Gallet, J.C., Johnsen, S., Leuenberger, M., Loulergue, L., Luethi, D., Oerter, H., Parrenin, F., Raisbeck, G., Raynaud, D., Schilt, A., Schwander, J., Selmo, E., Souchez, R., Spahni, R., Stauffer, B., Steffensen, J.P., Stenni, B., Stocker, T.F., Tison, J.L., Werner, M., Wolff, E.W., 2007. Orbital and millennial Antarctic climate variability over the past 800,000 years. Science 317, 793-796.

Jullien, E., Grousset, F., Malaizé, B., Duprat, J., Sanchez-Goni, M.F. Eynaud, F., Charlier, K., Schneider, R., Bory, A., Bout, V., Flores, J.A., 2007. Low-latitude "dusty events" vs. high-latitude "icy Heinrich events". Quaternary Research 68, 3, 379-386.

Kallel, N., Paterne, M., Duplessy, J.C., Vergnaud-Grazzini, C., Pujol, C., Labeyrie, L., Arnold, M., Fontugne, M., Pierre, C., 1997. Enhanced rainfall in the Mediterranean region during the last sapropel event. Oceanologica Acta 20, 697– 712.

Kandiano, E.S., Bauch, H.A., 2007. Phase relationship and surface water mass change in the NorthEast Atlantic duringMarine Isotope stage 11 (MIS11). Quaternary Research 68, 445-455.

Kandiano, E.S., Bauch, H.a., Fahl, K., Helmke, J P., Röhl, U., Pérez-Folgado, M., Cacho, I., 2012. The meridional temperature gradient in the eastern North Atlantic during MIS11 and its link to the ocean–atmosphere system. Palaeogeography, Palaeoclimatology, Palaeoecology 333-334, 24-39..

Kawahata, H., 2005. Stable isotopic composition of two morphotypes of *Globigerinoides ruber* (white) in the subtropical gyre in the north Pacific. Paleontological Research 9 (1), 27-35.

Klein, P., Coste, P., 1984. Effects of wind stress variability on nutrient transport into the mixed layer. Deep-Sea Research 31, 21-37.

Konijnendijk, T.Y.M., Ziegler, M., Lourens, L.J., 2014. Chronological constraints on Pleistocene sapropel depositions from high-resolution geochemical records of ODP Sites 967 and 968. Newsletters on Stratigraphy 47 (3), 263-282.

Koutsodendris, A., Pross, J., Zahn, R., 2014. Exceptional Agulhas leakage prolonged interglacial warmth during MIS 11c in Europe. Paleoceanography 29, 1062-1071.

Krom, M.D., Kress, N., Brenner, S., Gordon, L.I., 1991. Phosphorus limitation of primary production in the eastern Mediterranean Sea. Limnology and ~~oceanography~~ Oceanography 36, 424-432.

Krom, M.D., Brenner, N.K., Neori, A., Gordon, L.I., 1992. Nutrient dynamics and new production in a warmcore eddy from the Eastern Mediterranean Sea. Deep-Sea Research 39, 467-480.

Krom, M.D., Thingstad, T.F., Brenner, S., Carbo, P., Drakopoulos, P., Fileman, T.W., Flaten, G.A.F., Groom, S., Herut, B., Kitidis, V., Kress, N., Law, C.S., Liddicoat, M.I., Mantoura, R.F.C., Pasternak, A., Pitta, P., Polychronaki, T., Psarra, S., Rassoulzadegan, F., Skjoldal, E.F., Spyres,

G., Tanaka, T., Tselepides, A., Wassmann, P., Wexels Riser, C.,Woodward, E.M.S., Zodiatis, G., Zohary, T., 2005. Summary and overview of the CYCLOPS P addition Lagrangian experiment in the Eastern Mediterranean. Deep-Sea Research II 52, 3090–3108.

Krom, M.D., Emeis, K.C., Van Cappellen, P., 2010. Why is the Eastern Mediterranean phosphorus limited? Progress in Oceanography 85, 236–244.

Kucera, M., 2007. Planktonic foraminifera as tracers of past oceanic environments. In: Hillaire-Marcel, C. and de Vernal, A. (eds): Developments in Marine Geology, Volume 1, Proxies in late Cenozoic. Paleoceanography. Elsevier, ISBN 13: 9780444527554~~.~~, pp. 213-262.

Kuroyanagi, A., Kawahata H., 2004. Vertical distribution of living planktonic foraminifera in the seas around Japan. Marine Micropaleontology 53, 173-196.

Kuroyanagi, A., Tsuchiya, M., Kawahata, H., Kitazato, H., 2008. The occurrence of two genotypes of the planktonic foraminifer *Globigerinoides ruber* (white) and paleoenvironmental implications. Marine Micropaleontology 68, 236-243.

Langereis, C.G., Dekkers, M.J., De Lange, G.J., Paterne, M., Van Santvoort, P. J. M., 1997. Magnetostratigraphy and astronomical calibration of the last 1.1 Myr from an eastern Mediterranean piston core and dating of short events in the Brunhes. Geophysical Journal International 129, 75-94.

Laskar, J., Robutel, P., Joutel, F., Gastineau, M., Correia, A.C.M., Levrard, B., 2004. A Long-term Numerical Solution for the Insolation Quantities of the Earth: Astronomy and Astrophysics 428, 261- 285.

Lin, H.L., Wang, W.C., Hung, G.W., 2004. Seasonal variation of planktonic foraminiferal isotopic composition from sediment traps in the South China Sea. Marine Micropaleontology 53 (3-4), 447–460.

Lin, H.L., Hsieh, H.Y., 2007. Seasonal variations of modern planktonic foraminifera in the South China Sea. Deep Sea Research Part II: Tropical Studies in Oceanography 54, 1634-1644.

Lionello, P., Malanotte-Rizzoli, P., Boscolo, R., Alpert, P., Artale, V., Li, L., Luterbacher, J., May, W., Trigo, R., Tsimplis, M., Ulbrich, U., Xoplaki, E., 2006. The Mediterranean climate: an overview of the main characteristics and issues. In: Lionello, P., Malanotte-Rizzoli, P., Boscolo, R. (Eds.), Mediterranean Climate Variability. Elsevier, Amsterdam, The Netherlands, pp. 1-26.

Lirer, F., Sprovieri, M., Ferraro, L., Vallefuoco, M., Capotondi, L., Cascella, A., Petrosino, P., Insinga, D., Pelosi, N., Tamburrino, S., Lubritto, C., 2013. Integrated stratigraphy for the Late Quaternary in the eastern Tyrrhenian Sea. Quaternary International 292, 71-85.

Lirer, F., Sprovieri, M., Vallefuoco, M., Ferraro, L., Pelosi, N., Giordano, L., Capotondi, L., 2014. Planktonic foraminifera as bio-indicators for monitoring the climatic changes occurred during the last 2000 years in the SE Tyrrhenian Sea. Integrative Zoology Journal 9, 542–554. Lisiecki, L.E., Raymo, M.E., 2005. A Pliocene–Pliestocene stack of 57 globally distributed benthic d18O records. Paleoceanography 20, PA1003. doi:10.1029/2004PA001071.

Lisiecki, L.E., Raymo, M.E., 2005. A Pliocene–Pliestocene stack of 57 globally distributed benthic d18O records. Paleoceanography 20, PA1003. doi:10.1029/2004PA001071.

Loewemark, L., Hong, W.L., Yui, T.F., Hung, G.W., 2005. A test of different factors influencing the isotopic signal of planktonic foraminifera in surface sediments from the northern South China Sea. Marine Micropaleontology 55/1–2, 49–62.

Lourens, L.J., Hilgen, F.J., Zachariasse, W.J., van Hoof, A.A.M., Antonarakou, A., Vergnaud-Grazzini, C., 1996a. Evaluation of the plio-Pleistocene astronomical time scale. Paleoceanography 11, 391– 413.

Lourens, L.J., Hilgen, F.J., Raffi, I., Vergnaud-Grazzini, C., 1996b. Early Pleistocene chronology of the Vrica section (Calabria, Italia). Paleoceanography 11, 797– 812.

Lourens, L.J., 2004. Revised tuning of Ocean Drilling Program Site 964 and KC01B (Mediterranean) and implications for the d18O, tephra, calcareous nannofossil, and geomagnetic reversal chronologies of the past 1.1 Myr. Paleoceanography 19, PA3010.

Loutre, M.F., 2003. Clues from MIS11 to predict the future climate — a modelling point of view. Earth and Planetary Science Letters 212, 213-224.

Luterbacher, J., Xoplaki, E., 2005. 500-year winter temperature and precipitation variability over the Mediterranean area and its connection to the large-scale atmospheric circulation. In: Bolle, H.-J. (Eds.) Mediterranean Climate. Variability and Trends. Springer Verlag, Berlin, New York, pp. 133-153.

Maiorano, P., Tarantino, F., Marino, M., De Lange, G. J., 2013. Paleoenvironmental conditions at Core KC01B (Ionian Sea) through MIS13–9: Evidence from calcareous nannofossil assemblages. Quaternary International 288, 97-111.

Malanotte-Rizzoli, P., Bergamasco, A., 1991. The wind and thermally driven circulation of the eastern Mediterranean Sea. Part II: The baro- clinic case. Dynamics of atmospheres and oceans 15, 355–419, doi:10.1016/0377-0265(91)90026-C.

Malanotte-Rizzoli, P., Artale, V., Borzelli-Eusebi, G.L., Brenner, S., Crise, A., Gacic, M., Kress N., Marullo, S., Ribera d'Alcalà, M., Sofianos, S., Tanhua, T., Theocharis, A., Alvarez, M., Ashkenazy, Y., Bergamasco, A., Cardin, V., Carniel, S., Civitarese, G., D'Ortenzio, F., Font, J., Garcia-Ladona, E., Garcia-Lafuente, J.M., Gogou, A., Gregoire, M., Hainbucher, D., Kontoyannis, H., Kovacevic, V., E. Kraskapoulou, G. Kroskos, Incarbona, A., Mazzocchi, M.G., Orlic, M., Ozsoy E., Pascual, A., Poulain, P. M., Roether, W., Rubino, A., Schroeder, K., Siokou-Frangou, J., Souvermezoglou, E., Sprovieri, M., Tintoré, J., Triantafyllou, G., 2014. Physical forcing and physical/biochemical variability of the Mediterranean Sea: a review of unresolved issues and directions for future research. Ocean Science 10, 281–322.

Manca, B., Burca, M., Giorgetti, A., Coatanoan, C., Garcia, M.J., Iona, A. 2004. Physical and biochemical averaged vertical profiles in the Mediterranean regions: an important tool to trace the climatology of water masses and to validate incoming data from operational oceanography. Journal of Marine Systems -48, 83-116.

Marino, G., Rohling, E.J., Rodrìguez-Sanz, L., Grant, K.M., Heslop, D., Roberts, A.P., Stanford, J.D., Yu, J., 2015. Bipolar seesaw control on last interglacial sea level. Nature 522, 197.

Martrat, B., Grimalt, J.O., Lopez-Martinez, C., Cacho, I., Sierro, F.J., Flores, J.A., Zahn, R., Canals, M., Curtis, J. H., Hodell, D.A., 2004. Abrupt temperature changes in the western Mediterranean over the past 250,000 years. Science 306, 1762–1765.

Masson-Delmotte, V., Kageyama, M., Braconnot, P., Charbit, S., Krinner, G., Ritz, C., Guilyardi, E., Jouzel, J., Abe-Ouchi, A., Crucifix, M., Gladstone, R.M., Hewitt, C.D., Kitoh, A., LeGrande, A.N., Marti, O., Merkel, U., Motoi, T., Ohgaito, R., Otto-Bliesner, B., Peltier, W.R., Ross, I., Valdes, P.J., Vettoretti, G., Weber, S.L., Wolk, F., Yu, Y., 2006. Past and future polar amplification of climate change: climate model intercomparisons and ice-core constraints. Climate Dynamics 26, 513-529.

McManus, J.F., Oppo, D.W., Cullen, J.L., 1999. A 0.5 million year record of millennial-scale climate variability in the North Atlantic. Science 283, 971-974.

Milker, Y., Rachmayani, R., Weinkauf, M.F.G., Prange, M., Raitzsch, M., Schulz, M., Kucera, M., 2013. Global and regional sea surface temperature trends during Marine Isotope Stage 11. Climate of the Past 9, 2231- 2252.

Moreno, A., Cacho, I., Canals, M., Prins, M. A., Sánchez-Goñi, M. F., Grimalt, J. O., and Weltje, G. J., 2002. Saharan dust transport and high latitude glacial climatic variability: the Alboran Sea record. Quaternary Research 58, 318-328.

Myers, P.G., Haines, K., Rohling, E.J., 1998. Modelling the paleo-circulation of the Mediterranean: the last glacial maximum and the Holocene with emphasis on the formation of sapropel S1. Paleoceanography 13, 586-606.

Napolitano, E., Oguz, T., Malanotte-Rizzoli, P., Yilmaz, A., Sansone, E., 2000. Simulations of biological production in the Rhodes and Ionian basins of the eastern Mediterranean. Journal of Marine Systems 24, 277-298.

Negri, A., Capotondi, L., Keller, J., 1999. Calcareous nannofossils, planktonic foraminifera and oxygen isotopes in the late Quaternary sapropels of the Ionian Sea. Marine Geology, 157: 89-103.

Numberger, L., Hemleben, C., Hoffmann, R., Mackensen, A., Schulz, H., Wunderlich, J.-M., Kucera, M., 2009. Habitats, abundance patterns and isotopic signals of morphotypes of the planktonic foraminifer Globigerinoides ruber (d'Orbigny) in the eastern Mediterranean Sea since the Marine Isotopic Stage 12. Marine Micropaleontology 73 (1-2), 90-104.

Olausson, E., 1991. A post-Cromerian rise in sea level. In: Weller, G., Wilson, C.L., Severin, B.A.B. (Eds.), International Conference on the Role of Polar Regions in Global Change: Proceedings of a Conference Held Jun 11–15, 1990 at the University of Alaska Fairbanks vol. II. Geophysical Inst. Univ. of Alaska Fairbanks, pp. 496–498.

Oppo, D.W., McManus, J.F., Cullen, J.L., 1998. Abrupt climate events 500 000 to 340 000 years ago: evidence from subpolar North Atlantic sediments. Science 279, 1335-1338.

Perez-Folgado, M, Sierro, F.J., Flores, J.A., Cacho, I., Grimalt, J.O., Zahn, R., Shackleton, N.J., 2003. Western Mediterranean planktonic foramini- fera events and millennial climatic variability during the last 70kyr. Marine Micropaleontology 48, 49-70.

Petit, J.R., Jouzel, J., Raynaud, D., Barkov, N.I., Barnola, J.M., Basile, I., Bender, M., Chappellaz, J., Davis, J., Delaygue, G., Delmotte, M., Kotlyakov, V.M., Legrand, M., Lipenkov, V., Lorius, C., Pépin, L., Ritz, C., Saltzman, E., Stievenard, M., 1999. Climate and atmospheric history of the past 420,000 years from the Vostok Ice Core, Antarctica. Nature 399, 429-436.

899 Pierre, C., Belanger, P., Saliège, J.F., Urrutiaguer, M. J., Murat, A., 1999. Paleoceanography of the
900 western Mediterranean during the Pleistocene: Oxygen and carbon isotope records at Site 975,
901 Proceedings of the Ocean Drilling Program, Scientific Results 161, 481–488.

902 Pinardi, N., Masetti, E., 2000. Variability of the large-scale general circulation of the Mediterranean
903 Sea from observations and mod- elling: a review. Palaeogeography Palaeoclimatology
904 Palaeoecology 158, 153-173.

905 Piva, A., Asioli, A., Trincardi, F., Schneider, R. R., Vigliotti, L., 2008. Late-Holocene climate
906 variability in the Adriatic Sea (Central Mediterranean). The Holocene 18 (1), 153-167.

907 Pujol, C., Vergnaud-Grazzini, C., 1989. Palaeoceanography of the last deglaciation in the Alboran
908 Sea (western Mediterra- nean): Stable isotopes and planktonic foraminiferal records. Marine
909 Micropaleontology 15, 153-179.

910 Pujol, C., Vergnaud-Grazzini, C., 1995. Distribution patterns of live planktonic foraminuifers as
911 related to regional hydrography and productive system of the Mediterranean Sea. Marine
912 Micropaleontology 25, 187-217.

913 Reynolds, l.A., Thunell, R.C., 1986. Seasonal production and morphologic variation of
914 Neogloboquadrina pachyderma (Ehrenberg) in the northeast Pacific: Micropaleontology 32, 1–18.

915 Roberts, A. P., Rohling E. J,. Grant, K. M.,. Larrasoaña, J. C., Liu, Q., 2011. Atmospheric dust
916 variability from Arabia and China over the last 500,000 years. Quaternary Science Reviews, 30,
917 3537-3541.

918 Robinson, A.R., Golnaraghi, M., Leslie, W.G., Artegiani, A., Hecht, A., Lazzoni, E., Michelato, A.,
919 Sansone, E.A., Theocharis, A., Unluata, U., 1991. Structure and variability of the Eastern
920 Mediterranean general circulation. Dynamics of Atmospheres and Oceans 15, 215-240.

921 Rodrigues, T., Voelker, A.H.L., Grimalt, J.O., Abrantes, F., Naughton, F., 2011. Iberian Margin sea
922 surface temperature during MIS15 to 9 (580–300 ka): glacial suborbital variability versus
923 interglacial stability. Paleoceanography 26, PA1204, doi.:10.1029/2010PA001927.

924 Roether, W.H., Manca, B.B., Klein, B., Bregant, D., Georgopoulos, D., Beitzel, V., Kovacevic, V.,
925 Luchetta, A., 1996. Recent changes in eastern Mediterranean deep waters. Science 271, 333-335.

926 Rogerson, M., Cacho, I., Jimenez-Espejo, F., Reguera, M.I., Sierro, F.J., Martinez-Ruiz, F., Frigola,
927 J., Canals, M., 2008. A dynamic explanation for the origin of the western Mediterranean organic-
928 rich layers. Geochemistry, Geophysics, Geosystems 9, Q07U01. doi:10.1029/2007GC001936.

929 Rohling, E.J., Gieskes, W.W.C., 1989. Late Quaternary changes in Mediterranean intermediate
930 water density and formation rate. Paleoceanography 4, 531–545.

931 Rohling, E.J., 1991. A simple two-layered model for shoaling of the eastern Mediterranean
932 pycnocline due to glacio-eustatic sea level lowering. Paleoceanography 6, 537–541.

933 Rohling, E.J., Jorissen, F.J., Vergnaud-Grazzini, C., Zachariasse, W.J., 1993. Northern Levantine
934 and Adriatic Quaternary planktic foraminifera; Reconstruction of paleoenvironmental gradients.
935 Marine Micropaleontology 21, 191-218.

936 Rohling, E.J., 1994. Review and new aspects concerning the formation of eastern Mediterranean
937 sapropels. Marine Geology 122, 1-28.

938 Rohling, E.J., Fenton, M., Jorissen, F.J., Bertrandt, P., Gans- sen, G., Caulet, J.P., 1998.
939 Magnitudes of sea-level low- stands of the past 500,000 years. Nature 394, 162-164.

940 Rohling, E.J., De Rijk, S., 1999. The Holocene Climate Optimum and Last Glacial Maximum in the
941 Mediterranean: The marine oxygen isotope record. Marine Geology 153, 57-75.

942 Rohling, E.J., Grant, K., Bolshaw, M., Roberts, A.P., Siddall, M., Hemleben, Ch, Kucera, M., 2009.
943 Antarctic temperature and global sea level closely coupled over the past five glacial cycles. Nature
944 Geoscience 2, 500-504.

945 Rohling, E.J., Foster, G.L., Grant, K.M., Marino, G., Roberts, A.P., Tamisiea, M.E., Williams, F.,
946 2014. Sea-level and deep-sea-temperature variability over the past 5.3 million years. Nature 508,
947 477–482.

948 Rohling, E. J., Marino, G., Grant, K. M., 2015. Mediterranean climate and oceanography, and the
949 periodic development of anoxic events (sapropels). Earth-Science Reviews 143, 62–97.

950 Rossignol-Strick, M., 1983. African monsoons, an immediate climate response to orbital insolation.
951 Nature 30, 446–449.

952 Rossignol-Strick, M., Paterne, M., Bassinot,F., Emeis,K.-C., DeLange,G.J., 1998. An unusual mid-
953 Pleistocene monsoon period over Africa and Asia. Nature 392, 269-272.

954 Rossignol-Strick, M., Paterne M., 1999. A synthetic pollen record of the eastern Mediterranean
955 sapropels of the last 1 Ma: Implications for the time-scale and formation of sapropels. Marine
956 Geology 153, 221–237.

957 Sanvoisin, R., D'Onofrio, S., Lucchi, R., Violanti, D., Castradori, D., 1993. 1 Ma Paleoclimatic
958 record from the Eastern Mediterranean Marflux Project: the first results of
959 micropaleontological and sedimentological investigation of a long piston core from the
960 Calabrian Ridge. Il Quaternario 6, 169–188.

961 Sarmiento, J., Herbert, T., Toggweiler, J.R., 1988. Mediterranean nutrient balance and episodes of
962 anoxia. Global Biogeochemical Cycles 2, 427-444.

963 Schiebel, R., Waniek, J.J., Matthias, B., Hemleben, C., 2001. Planktic foraminiferal production
964 stimulated by chlorophyll redistribution and entrainment of nutrients. Deep Sea Research Part I.
965 Oceanographic Research Papers 48 (3), 721-740.

966 Schneider, T., Bischoff, T., Haug, G.H., 2014. Migrations and dynamics of the intertropical
967 convergence zone. Nature 513, 45–53.

968 Seguenza, G., 1880. Le formazioni terziarie nella provincia di Reggio (Calabria): Rendiconti
969 Accademia dei Lincei, CI. Sci. Fis. Mat. Nat., Mem., ser. 3, v.6, 3-446, tav. 1-17.

970 Shackleton, N.J., 1987. Oxygen isotopes, ice volume and sea level. Quat. Sci. Rev. 6, 183-190.

971 Siani, G., Paterne, M., Colin, C., 2010. Late Glacial to Holocene planktonic foraminifera bioevents
972 and climatic record in the South Adriatic Sea, Journal of Quaternary Science 25, 808–821.

973 Siegenthaler U., Stocker T.F., Monnin E., Luethi D., Schwander J., Stauffer B., Raynaud D., et al.,
974 2005. Stable carbon cycle-climate relationship during the late Pleistocene. Science 310, 1313-
975 1317.

Sierro F.J., Flores, J.A., –Frances,G., Vazquez, A., Utrilla, R., –Zamarreno, I., –Erlenkeuser, H.,. Barcena, M.A., 2003. Orbitally-controlled oscillations in planktic communities and cyclic changes in western Mediterranean hydrography during the Messinian. Palaeogeography, Palaeoclimatology, Palaeoecology 190, 289-316.

Sierro, F.J., Hodell, D.A., Curtis, J.H., Flores, J.A., Reguera, I., Colmenero-Hidalgo, E., Bárcena, M.A., Grimalt, J.O., Cacho, I., Frigola, J., Canals, M., 2005. Impact of iceberg melting on Mediterranean thermohaline circulation during Heinrich events. Paleoceanography 20, PA2019, -doi:10.1029/2004PA001051.

Sprovieri, R., Di Stefano, E., Incarbona, A., Gargano, M.E., 2003. A high- resolution record of the last deglaciation in the Sicily Channel based on foraminifera and calcareous nannofossil quantitative distri-bution. Palaeogeography, Palaeoclimatology, Palaeoecology 202, 119–142.

Sprovieri, M., Di Stefano, E., Incarbona, A., Salvagio Manta, D., Pelosi, N., Ribera d'Alcalà, M., Sprovieri, R., 2012. Centennial to millennial scale climate oscillations in the Central Eastern Mediterranean Sea between 20,000 and 70,000 years ago: evidence from a high-resolution geochemical and micropaleontological record. Quaternary Science Reviews 46, 126-135.

Stefanelli, S., Capotondi, L., Ciaranfi, N., 2005. Foraminiferal record and environmental changes during the deposition of the early- middle Pleistocene sapropels in southern Italy. Palaeogeography, Palaeoclimatology, Palaeoecology 216, 27–52.

Stein, R., Hefter, J., Grützner, J., Voelker, A., Naafs, B.D.A., 2009. Variability of surface water characteristics and Heinrich-like events in the Pleistocene midlatitude North Atlantic Ocean: biomarker and XRD records from IODP Site U1313 (MIS16-9). Paleoceanography 24, doi:10.1029/2008PA001639.

Thirumalai, K., Richey, J.N., Quinn, T.M., Poore, R.Z., 2014. Globigerinoides ruber morphotypes in the Gulf of Mexico: A test of null hypothesis. Scientific Reports 4, 6018.

Thunell, R.C., 1978. Distribution of recent planktonic foraminifera in surface sediments of the Mediterranean Sea. Marine Micropaleontology 3, 147–173.

Thunell, R.C., Poli, M-S., Rio, D., 2002. Changes in deep and intermediate water properties in the western North Atlantic during marine isotope stages 11–12: evidence from ODP Leg 172, Marine Geology 189, 63–77.

Triantaphyllou, M.V., Ziveri, P., Gogou, A., Marino, G., Lykousis, V., Bouloubassi, I., Emeis, K.C., Kouli, K., Dimizia, M., Rosell-Mele, A., Papanikolaou, M., Katsouras, G., Nunez, N., 2009. Late GlacialeHolocene climate variability at the south-eastern margin of the Aegean Sea. Marine Geology 266, 182-197.

Trigo, R.M., Pozo-Vazquez, D., Osborn, T.J., Castro-Dıez, Y., Gamiz-Fortis, S., Esteban-Parra, M.J., 2004. North Atlantic oscillation influence on precipitation, river flow and water resources in the Iberian Peninsula. International Journal of Climatology 24, 925-944.

Tzedakis, P.C., 2010. The MIS 11—MIS 1 analogy, southern European vegetation, atmospheric methane and the early anthropogenic hypothesis. Climate of the Past 6, 131–144.

Tzedakis, P.C., Channell, J.E.T., Hodell, D.A., Kleiven, H.F., and Skinner, L.C., 2012a. Determining the natural length of the current interglacial. Nature Geoscience 5, 138–141.

Formatted: Justified

van Santvoort, P. J.M., De Lange, G.J., Langereis, C.G., Dekkers, M.J., 1997. Geochemical and paleomagnetic evidence for the occurrence of ‘‘missing’’ sapropels in eastern Mediterranean sediments, Paleoceanography 12 (6), 773-786.

Voelker, A.H.L., Rodrigues, T., Hefter, J., Billups, K., Oppo, D., McManus, J., Stein, R., Grimalt, J.O., 2010. Variations in mid-latitude North Atlantic surface water properties during the mid-Brunhes (MIS9–14) and their implications for the thermohaline circulation. Climate of the Past 6, 531-552.

Wang, L.J., 2000. Isotopic signals in two morphotypes of *Globigerinoides ruber* (white) from the South China Sea: implications for monsoon climate change during the last glacial cycle. Palaeogeography, Palaeoclimatology, Palaeoecology 161 (3–4), 381–394.

Wang, Y.J., Cheng, H., Edwards, R.L., An, Z.S., Wu, J.Y., Shen, C.C., Dorale J.A., 2001. A high-resolution absolute-dated late Pleistocene monsoon record from Hulu Cave, China. Science 294, 2236–2239.

Ziveri, P., Rutten, A., de Lange, G.J., Thomson, J., Corselli, C., 2000. Present-day coccolith fluxes recorded in central Eastern Mediterranean sediment traps and surface sediments. Palaeogeography, Palaeoclimatology, Palaeoecology 158, 175-195.

***Revision Notes**

Click here to download Revision Notes: RevisionNotes.doc

Responses to the reviewers

Reviewer #1

- I would like to highlight a list of typos throughout the manuscript (clean version): lines 50, 51, 54, 55, 58, 59, 63, 68, 70, 77, 79, 81, 83, 85, 86, 95, 100, 101, 106, 122, 125, 126, 128, 129, 137-139, 141-144, 147, 148, 153, 154, 175, 185, 189, 222-225, 228, 229, 238, 292, 297, 298, 304-306, 308, 314, 319, 321-325, 327, 330, 335, 339, 341, 344, 347, 351-353, 356, 359, 360, 371, 373, 400, 401, 410, 414, 415, 417, 419, 420, 422, 423, 430, 435, 439-442, 446, 449, 452, 456, 463-465, 467, 468, 474, 476-478, 485-488, 491, 495, 496, 499, 500, 505, 513, 521, 525, 535, 549, 556-558 and 562.

OK. Done.

Typing errors highlighted throughout the manuscript probably are due to the translation from the "file.word" to the "file.pdf" as I checked throughout the version".word" and they are not present. However, I did not understand why it happened. I think this is probably due to the fact that I have submitted the manuscript as a file "word.docx" and not "word.doc". Probably the system does not convert well the version “word.docx”.

- remove AMOC, the acronym was already cited.

OK. Done.

Reviewer #2

- I suggest that a native english speaker should get a last and fresh read over the manuscript

OK. Done.

Table1
Click here to download Table: Tab1.doc

Tie-point	Depth (mcd)	Age kyr	Reference
sapropel S'	15,74	287,5	Konijnendijk et al. (2014)
sapropel S10	16,84	332,3	Konijnendijk et al. (2014)
base MIS 9	17,15	337	Lisiecki and Raymo (2005)
sapropel S11	19,27	418,9	Konijnendijk et al. (2014)
base MIS 12	20,83	474	Lisiecki and Raymo (2005)
sapropel S12	21,74	504,5	Konijnendijk et al. (2014)

Tab. 1 - Tie-points used in this work for the construction of the age model

Figure1

Click here to download high resolution image

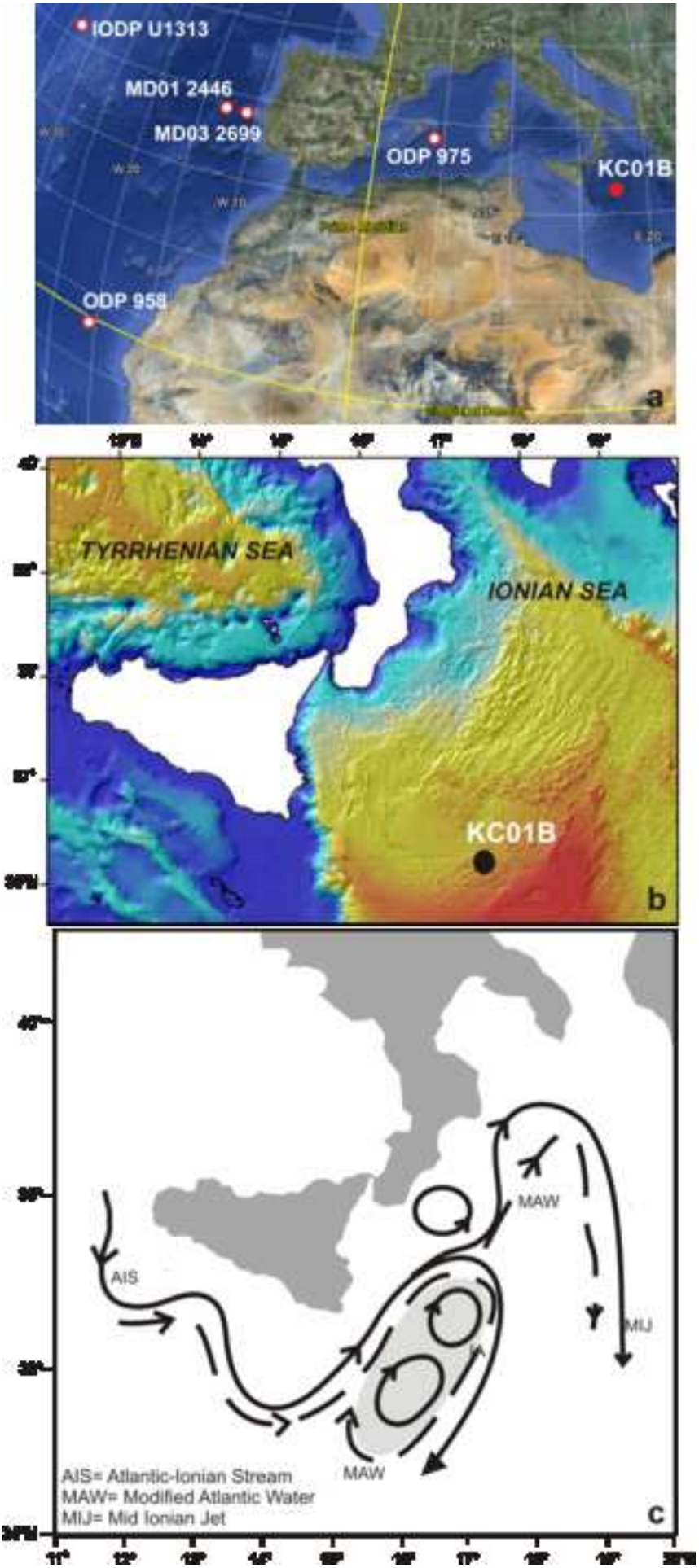

Figure2

Click here to download high resolution image

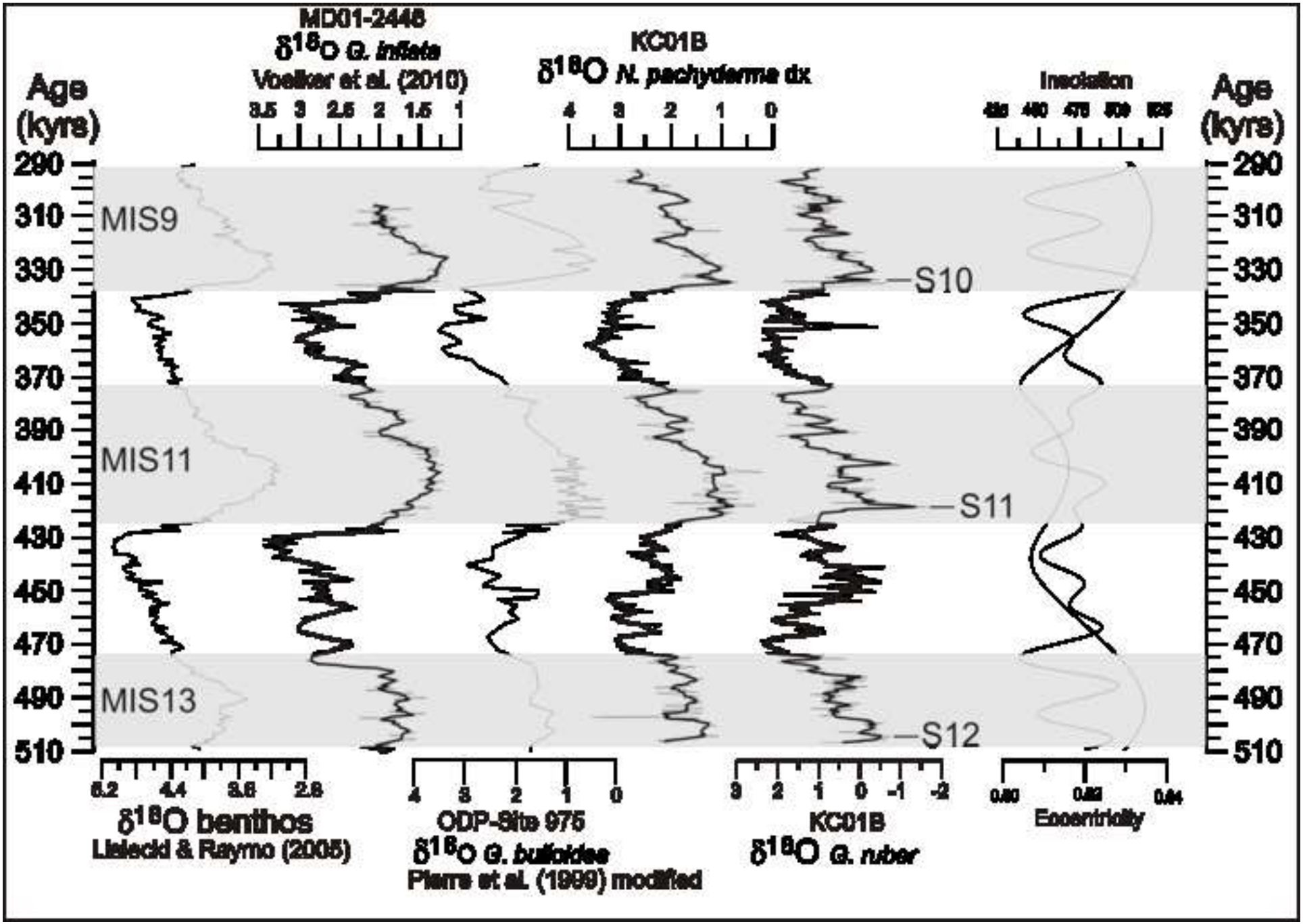

Figure3

Click here to download high resolution image

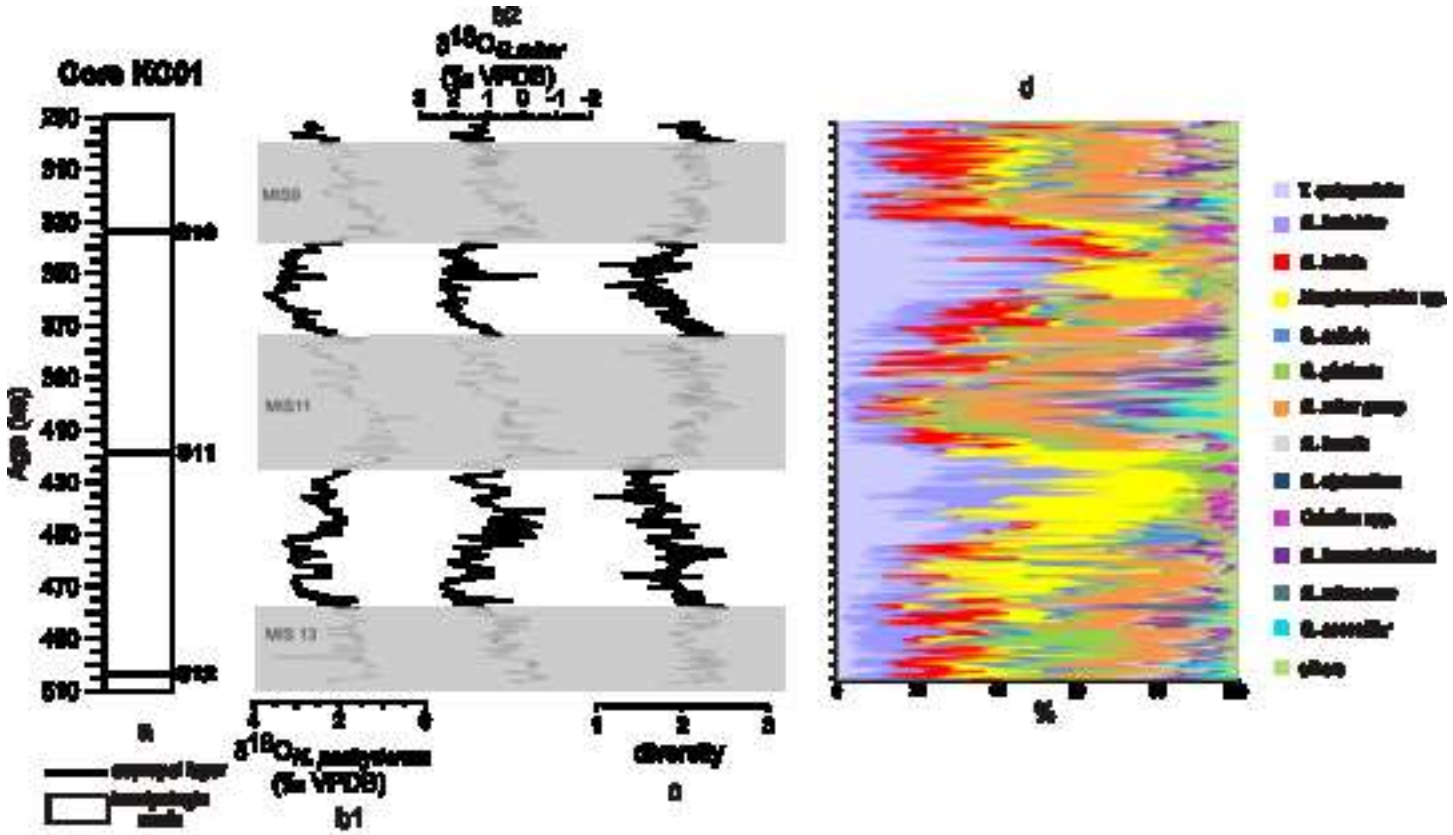

Figure4

Click here to download high resolution image

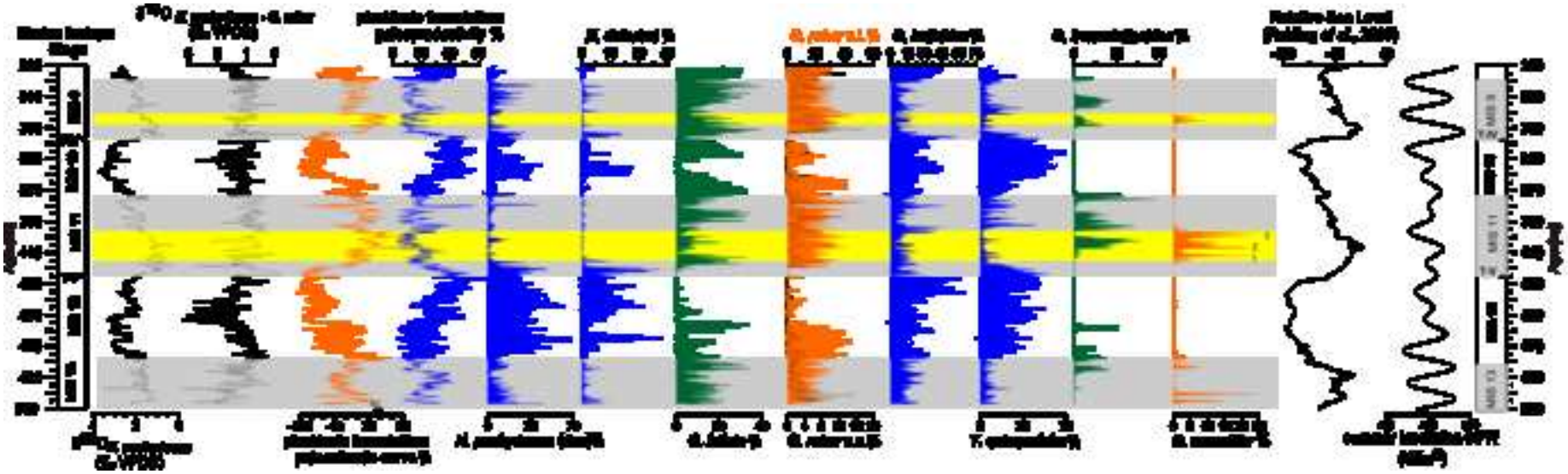

Figure5

Click here to download high resolution image

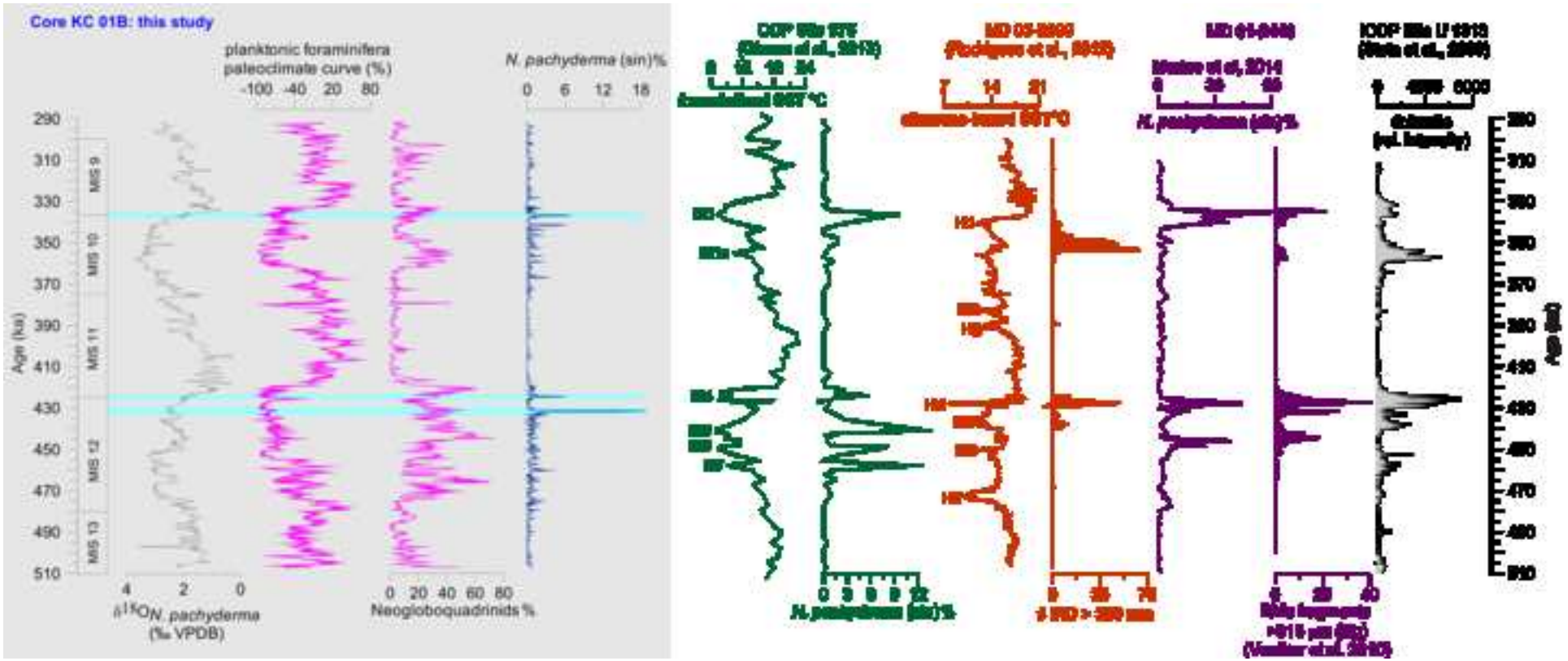

Figure6

Click here to download high resolution image